China Active Faults Database (CAFD) and its Web System

Xiyan Wu[1], Xiwei Xu[2,3], Guihua Yu[1], Junjie Ren[3], Xiaoping Yang[1], Guihua Chen[1], Chong Xu[3], Keping Du[4], Xiongnan Huang[1], Haibo Yang[1], Kang Li[3], Haijian Hao[1]

[1] State Key Laboratory of Earthquake Dynamics, Institute of Geology, China Earthquake Administration, Beijing 100029, China
[2] School of Earth Sciences and Resources, China University of Geosciences, Beijing 100083, China
[3] National Institute of Natural Hazards, Ministry of Emergency Management of China, Beijing, 100085, China
[4] Beijing Normal University, Beijing100091, China

Correspondence to: Xiwei Xu (xiweixu@vip.sina.com)

Abstract. Active faults serve as potential sources of destructive earthquakes. Studies and investigations of active faults are necessary for earthquake disaster prevention. This study presents a nation-scale database of the active faults in China and its adjacent regions in tandem with an associated web-based query system. This database is an updated version of the active faults data included in the "Seismotectonic Map of China and its Adjacent Regions (1:4 000 000)," which is one of the four essential maps of the mandatory Chinese standard GB/T 18306-2015 Seismic Ground Motion Parameter Zonation Maps of China. The data update and integration stem from regional-scale studies and surveys conducted over the past two decades (at reference scales from 1:250,000 to 1:50,000). The information amassed from these regional-scale studies and surveys encompasses geophysical probing, drill logging, measurement of offset-landform, sample dating, as well as geometric and kinematic parameters of exposed and blind faults, paleo-earthquake sequences, and recurrence intervals. These data have been acquired and analyzed utilizing a uniform technical standard framework and reviewed by expert panels in both field and laboratory settings. Our system hosts this nation-scale database accessible through a Web Geographic Information System (GIS) application, enabling browsing, quiring, and downloading functionalities via a web browser. The system we built also publishes the Open Geospatial Consortium (OGC) Web Feature Service and OGC Web Map Service of active fault data. Users can incorporate map layers and obtain fault data in OGC-compliant GIS software for further analysis through these services. The Chinese government, research institutions, and companies have widely used the active faults data from the previous versions of the Database. The database is available at https://doi.org/10.12031/activefault.china.400.2023.db (Xu, 2023) and via the Web System (CEFIS (V2), 2023; CAFD WFS).

1 Introduction

30   Earthquake is one of the most dangerous natural disasters in the world. A causative relationship exists between large or great earthquakes and active faults. Typically, earthquakes with magnitude (M) ≥ 7.0 often originate from Holocene or Late Pleistocene active faults or their epicentral zone overlaps such faults. Statistical analyses reveal that nearly all earthquakes with M≥ 8.0 and the majority of those ranging from 7.0 to 7.9 in China are linked to rupture segments of the primary boundary faults surrounding the Tibetan Plateau block in western China and the Ordos block in Central and East China (Xu

35   and Deng, 1996; Deng et al., 2003; Zhang et al., 2003; Xu et al., 2016a). Moreover, over 70 co-seismic surface rupture zones resulting from large earthquakes align spatially with known active faults (Xu and Deng, 1996; Zhang et al., 2003; Xu et al., 2017). Hence, the identification of active faults, delineation of their traces and locations,determination of their slip rates, and subsequent compilation of a comprehensive corresponding database are imperative for averting and mitigating the social and economic ramifications of earthquakes, as well as safegarding lives and property (Xu et al., 2002, 2006; Tian et al., 2006).

40   This article introduces a publicly accessible, national-scale database detailing fault traces, latest active ages, and motion modes of active faults in China.

    Several countries have compiled comprehensive active faults databases over the past two decades (Haller et al., 2004; Basili et al., 2008, 2021; Yoshioka and Miyamoto, 2011; Ganas et al., 2013; Langridge et al., 2016; Emre et al., 2018, Maldonado et al., 2021; Williams et al., 2022), some of which are available to the public. For instance, the National Institute of

45   Geophysics and Volcanology of Italy published the Database of Individual Seismogenic Source (DISS) in the 2000s and the database of Active and Capable Faults in ITaly HAzard from CApable faults (ITHACA, 2024) project. The latest iteration of DISS, version 3.3.0 (Valensise and Pantatosti, 2001; Basili et al., 2008, 2021), includes ~200 faults. The U.S. Geological Survey established the first nationwide compilation of the U.S. Quaternary Faults and Folds Database in the early 2000s, containing ~2000 faults (Haller et al., 2004).

50   China is located in the convergence zone of the Indian, Eurasian, and Pacific Plates where many seismogenic active faults have developed, and becomes one of the countries with the most severe earthquake disasters at present and also in history. An active fault database of China is essential for conducting in-depth analyses of regional crustal kinematic characteristics, intraplate earthquake features, and earthquake disaster mitigation strategies. In the 2000s, the China Earthquake Administration developed a 1:4,000,000-scale active tectonic database (Qu, 2008), which wasderived from Deng's

55   1:4,000,000-scale active tectonic map and encompassed over 800 active faults and 48 active folds (Deng et al., 2002, 2007). It summarized research on active faults carried out in China before 2002 AD. However, numerous active faults remained inadequately identified or studied during that period. In the following years, subsequent field surveys focused on investigating active neotectonic and seismic activities within the Circum-Pacific and Himalayan-Mediterranean seismic zones in China. To determine the accurate fault trace and age of the latest re-activation of active fault, which is of capable

60   generating destructive earthquakes, a series of active fault surveys and mapping projects (Yang et al., 2018a, 2018b, 2020; Huang et al., 2021a, 2021b; Lei et al., 2008; Chai et al., 2011, Xu et al., 2015) has been launched since 2007 in China. These

projects consist of the following: 1) Fundamental maps and data collection for national earthquake hazard prevention, such as the 5th generation "Seismic ground motion parameters zonation map of China" (China mandatory standard GB/T 18306-2015). 2) Prospecting of active faults in urban regions and their earthquake risk assessments, such as "Urban active fault experimental prospecting" (2001–2003)(Pan et al., 2002; Wang et al., 2002) and "Seismo-active-fault prospecting technology system in China" (2004–2008) (Wang et al., 2004; Deng et al., 2007;). 3) seismo-active-fault survey and mapping, such as "The Himalayan Plan: active fault mapping at a scale of 1:50,000 in the north China tectonic region and along the North-South seismic zone" and "Earthquake risk assessment of active faults in the key earthquake surveillance and prevention areas". 4) Various other scientific researches. These projects systematically analyze published scientific literature, remote sensing data, field surveys, and dating samples from geological profiles, trenches, and boreholes to ascertain accurate geometric and activity kinematic parameters, as well as mechanical properties of the studied active faults (Xu et al., 2015). A professional panel then reviewed the obtained evidences and parameters and rechecked the final results of these four types projects.. In every project, an overall prospecting-and-surveying-process database is built to record all project data from beginning to end. Those project databases include data associated with the geophysical prospecting, drilling, offset-landform measuring and age dating (e.g., cosmogenic nuclides, OSL, ESR, or ^{14}C used for dating offset-landform, and OSL or ^{14}C used for dating dislocated-strata in trench), as well as geometric and kinematic parameters of exposed and blind faults, paleo-earthquakes, their occurrence ages and recurrence intervals. Data types within these regionwide databases comprise two-dimensional Geographic Information System (GIS) data, photographs, geological photos with interpreted faults and illustrations, geophysical prospecting data, copyrighted electronic literature, and scientific reports. By the conclusion of 2019, the cumulative data from these projects had amassed to 7 Terabytes.

The China Active Faults Database (CAFD) represents a comprehensive geospatial database consolidating the most reliable outcomes from the aforementioned projects, predicated on two fundamental databases with accuracies of 1:50,000 for single active fault mappings and 1:250,000 for regional active fault distributions. The publicly accessible web-based query system offers the latest iteration of China's active fault database (CEFIS (V2)). Section 2 introduces the history and development of nationwide active fault maps and databases in China. Data acquisition, resources, processing, compilation, and quality are discussed in Section 3. Additionally, Section 3.9 presents several classical application cases in are presented to underscore the extensive utility of the database. The construction, function, performance, and usage of the web-based active fault query system are described in Section 4. System users can peruse and query fault information, obtain data from the Web Feature Service (WFS) and Web Map Service (WMS) servers in GIS software (such as ArcGIS and QGIS), and add active faults as layers in their web applications.

2 Nationwide active fault maps and databases

Various organizations and experts have compiled the nationwide active tectonics and fault maps of China at different junctures. Each map summarized all of the research as much as possible before its publication date. Maps such as the

"Spatial distribution map of active tectonics and strong earthquakes in China (1:3,000,000)" (NEIZMT, 1976), "Map of the major tectonic-system activity and strong earthquakes epicenter distribution in China (1:6,000,000)" (NEIZMT, 1978), "Seismotectonic map of China (1:4,000,000)" (GICEA, 1979), and "Lithospheric dynamics map of China and adjacent sea area (1:4,000,000)" (Ma, 1987), systematically synthesized the latest research achievements up to their respective periods.

In the last decade, the most influential nationwide active fault maps have been "The Active Tectonic Map of China (1:4,000,000)" (Deng et al., 2007) and "Seismotectonic Map in China and its Adjacent Regions (1:4,000,000)" (SMCAR; Xu et al., 2016). Deng et al. (2007) has been widely disseminated among scientists, specialists, and the general public over the past 10 years, albeit not being available online. Its earlier version was integrated into the early version of Active Faults of Eurasia Database (Trifonov et al., 2004), an updated version of which was published in 2022 (Zelenin et al., 2022). Presently, the database is freely downloadable online (NEDC (sub-center in IG, CEA), 2023), and scientists have updated this map with new findings. For instance, Wu et al. (2018) compiled a "spatial distribution map of active faults in China and its adjacent sea areas (1:5,000,000) (2018)" by synthesizing publications in Chinese and English from the past decadal and 15-year research on active faults conducted by the Institute of Geomechanics in the Chinese Academy of Geological Sciences.

The SMCAR (Xu et al., 2016) is a subproject of the 5th generation "Seismic ground motion parameter zonation maps of China" and is one of the four essential maps of the Chinese mandatory standard GB/T 18306-2015. This standard aims to develop seismic design criteria for seismic-resistant design in various regions. The SMCAR collected the latest re-activation ages of faults from the previously introduced nationwide maps and some public or unpublic data. The SMCAR is now open to the public on the web system of the 5th generation "Seismic ground motion parameter zonation maps" (GB18306, 2023), and it has a geospatial database edition in addition to print and Joint Photographic Experts Group editions. This database integrates seismically active faults in China and adjacent regions and is also known as CAFD (2015). After geospatial correlation using remote sensing images in the WGS84 coordinate system, its spatial accuracy surpassed that of previous analogous maps and datasets. The fault data encompass fault attributes such as name, main characteristics, and faulting age. A simplified version is utilized in constructing a probabilistic seismic hazard model for Mainland China (Rong et al., 2020).

3 Latest version of China Active Faults Database

3.1 Active faults database compilation workflow

The CAFD (2023) presented in this paper, which is based on the most reliable results of the projects introduced in Section 1, is an updated version of the CAFD (2015). The compilation workflow of the database is illustrated in Fig. 1.

The data used to update the nationwide CAFD (2015) are obtained from 120 regional project databases and research on active fault, earthquake surface rupture investigations, and published literature in the past two decades. All these databases adhere to the same technological framework and are generated under well-established principles of active fault surveys (Sections 3.2-3.4), aligning with the technical requisites of the Chinese mandatory standard (GB/T 36072-2018). Each regional project database adheres to the identical data schema and standard as recommended by the China Earthquake

Administration (GB/T 36072-2018; DB/T 53-2013; DB/T 65-2016; DB/T 81-2020; DB/T 82-2020; DB/T 83-2020). All parameter values of the fault data are computed following systematic criteria and definitions (Section 3.7). Given the uniformity data definition, schema, and acquisition method, there exists no information disparity among these project databases. All data are processed using the same workflow. First, multiple-scale active fault data are extracted from different databases. Second, they are used to update the geometric shapes and attributes of the corresponding fault data in a nationwide database. Finally, the updated database (2023) is translated into English, adjusted for deployment, and released online (Sections 3.4 and 3.6).

The CAFD (2023) is a culmination of numerous surveys (Section 3.5) and research endeavors(Xu et al., 2008a, 2008b, 2009a, 2009b; Chen et al., 2009; Xu et al., 2014a, 2014b; Xu et al., 2000; He et al., 2013; Shu et al., 2016, 2020; Li et al., 2019), encapsulating the current state of the integrated knowledge derived from seismic fault surveys in China.
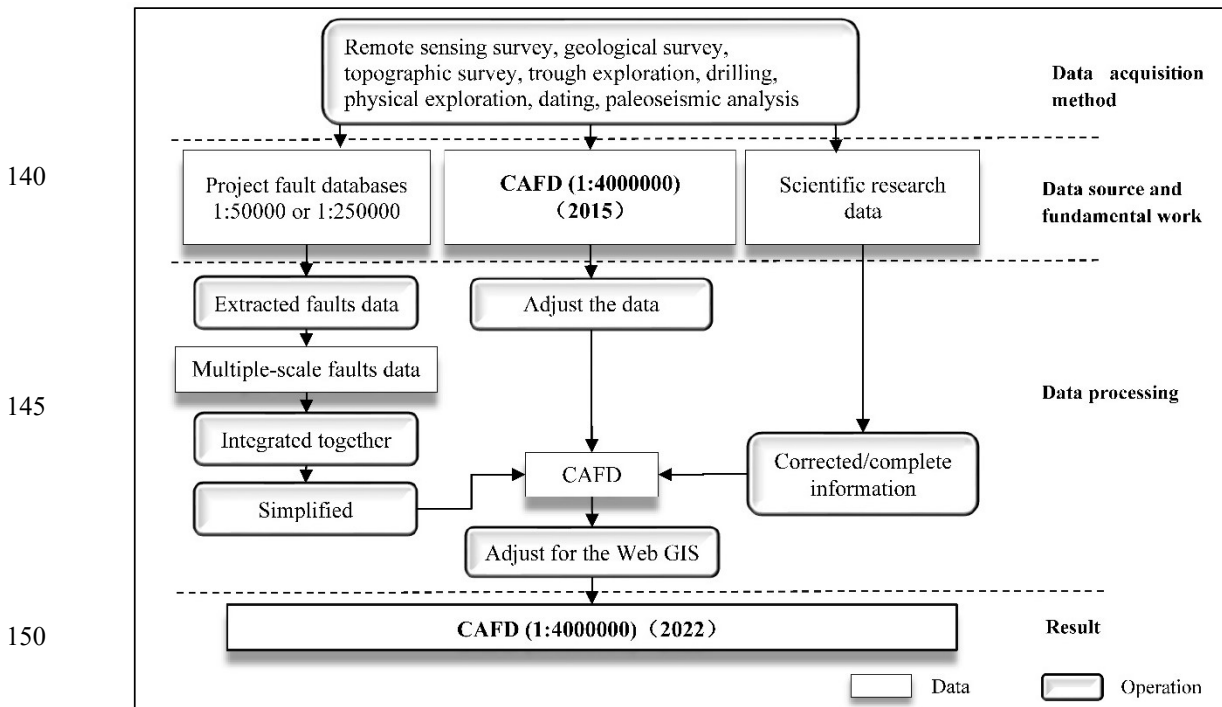
Figure 1: Workflow to construct the China Active Faults Database

3.2 Overview of data acquisition and methods

The location, motion type, and kinematic parameters of faults stored in the nationwide CAFD (2015)(1: 1,4,000,000) (Xu et al., 2016) and regional survey project databases (scale: 1:250,000–1:50,000), are acquired through a combination of methodologies including remote sensing data interpretation, geological field surveys, trenching, drilling, geophysical prospecting, dating, and paleo-seismic analysis. However, it's noteworthy that the nationwide CAFD (2015) exhibited

differing accuracies compared to the regional survey project databases. The horizontal accuracy of the nationwide database, on the scale of 1:4,000,000, is approximately 12.8 kilometers (GB/T 33178-2016). The nationwide CAFD (2015) (Xu et al., 2016) is based on previous studies. In earlier research, the low-resolution seismic petroleum exploration profiles caused the low accuracy of the interpreted top breakpoints. Because of that, the accuracy of positional precision of the blind faults was not precise. Additionally, limitations imposed by locator devices with lower positioning accuracy and reduced observation site density due to funding constraints further impacted positional accuracy. Conversely, survey mapping projects at scales of 1:50,000 exhibit a horizontal accuracy of 37.5 meters(GB/T 33177-2016), while urban active fault survey projects at 1:250,000 exhibit a horizontal accuracy of 200 meters (GB/T 33178-2016). The regional fault survey project databases (scale: 1:250,000–1:50,000) are based on quantitative methods written into the Chinese mandatory standard in 2018 (GB/T 36072-2018). These were classified as the exposed fault survey method (Section 3.3) and blind survey method (Section 3.4), and guaranteed a better data quality and accuracy than the nationwide CAFD (2015) (Xu et al., 2016).

3.3 Exposed fault survey method

The exposed faults are those with surface expressions (such as linear fault scarp, offset gullies, and folding) or fault outcrop. Within the contemporary fault database, we only strengthen the locations, kinematics, and ages of these near-surface faults. The fault geometry or dip angle, as suggested by seismic data, was not included. For the exposed faults with surface traces, remote sensing and Digital Elevation Model (DEM) data are initially utilized to map fault traces and generate an initial distribution map of active faults. Then, combined with the field surveys, the locations of the faults in this initial map are verified, corrected, and recorded. Finally, a systematic workflow that combines geomorphological surveys, stratigraphic analyses of the geological cross sections, trench stratigraphic logs, sample dating from terraces and trenches, and paleo-earthquake identification are used to obtain the latest faulting ages and kinematic parameters of the mapped active faults (DB/T 53-2013; Chen et al., 2016; Sun et al., 2017; Shi et al., 2019, 2022; Guo et al., 2021; Huang et al., 2021a). Within this workflow, accurately locating dislocated strata, samples, and trenches within typical offset landforms is crucial. The dislocated strata, visualized in the trench, reveal the number of paleo-earthquake events and the kinematics of faults. The ages of the dislocated strata, measured by dating methods, including radiocarbon (14C), cosmogenic nuclides (10Be), and luminescence techniques, determined the age of fault activity. These results were stored in those regional-scale survey databases.

The Fodongmiao-Hongyazi Fault, mapped at a scale of 1:50,000 (Yang et al., 2018a, 2018b, 2020; Huang et 180 al., 2021a, 2021b), serves as an example of the quantitative technical demands outlined in the Chinese mandatory standard (GB/T 36072-2018). First, remote sensing images with meter-level resolution (Quickbird, worldview, SPOT, etc.) and DEMs with horizontal and relative vertical resolutions of $\leqslant$ 37.5 m (SRTM 1 Arc-Second DEM, ARSTER-II DEM, etc.) were used to mark surface deformations or offset landforms (fault scarps, dislocated gullies, fault valleys, pull-apart basins, pressure ridges, terraces, alluvial or fluvial fans) and plan geological survey sites, lines, and areas. Following these marks and positions, the fault could be traced along its strike, and the coordinates of the exposed fault site are precisely recorded by

using Global Navigation Satellite System and hand-held GPS receivers. The average interval of coordinate-recording sites is 500–2 000 m, but if the surveyor can access a site, an interval of 500 m is required (Fig. 2; DB/T 53-2013). The density of the recorded sites controls the geometric accuracy of the fault data. The horizontal location error of every recorded site was less than 15 m. If the surface deformations or offset landforms disappear in some areas, the approximate fault location should be taken from the original interpretation of the high-resolution remote sensing images and DEM data. Subsequently, the next exposed fault segment is searched by traveling across the region in a "Z" route. When the next fault segment is identified again, the fault should be traced along its strike. After these steps, the geometry of the fault trace is finally confirmed on the map. Once the fault trace is ascertained, the fault is divided into segments based on the geological landforms, geometric structure (straight, curved, bent, etc.), displacement distribution, seismic rupture characteristics, or signs of fault activity, so that each section is relatively independent. Along the key segments, typical offset landforms should be selected for further geomorphic and topographic measurements (Fig. 3a & c). In every independent segment, dislocated strata, samples, and trenches are accurately located, and the number of paleo-earthquake events is visualized in the trenches (Fig. 3b and d). Dating of dislocated strata only provides maximal age of rupturing event. To get more reliable age of the event we have to date both ruptured and non-ruptuted units. Common dating methods include radiocarbon (^{14}C), cosmogenic nuclides (^{10}Be), and luminescence techniques. The fault is divided into segments based on the mapped geometry. The ages obtained from a single geometry segment presented the age of this segment. They are used to identify whether or not a fault is active, to calculate its slip rate during a certain period.
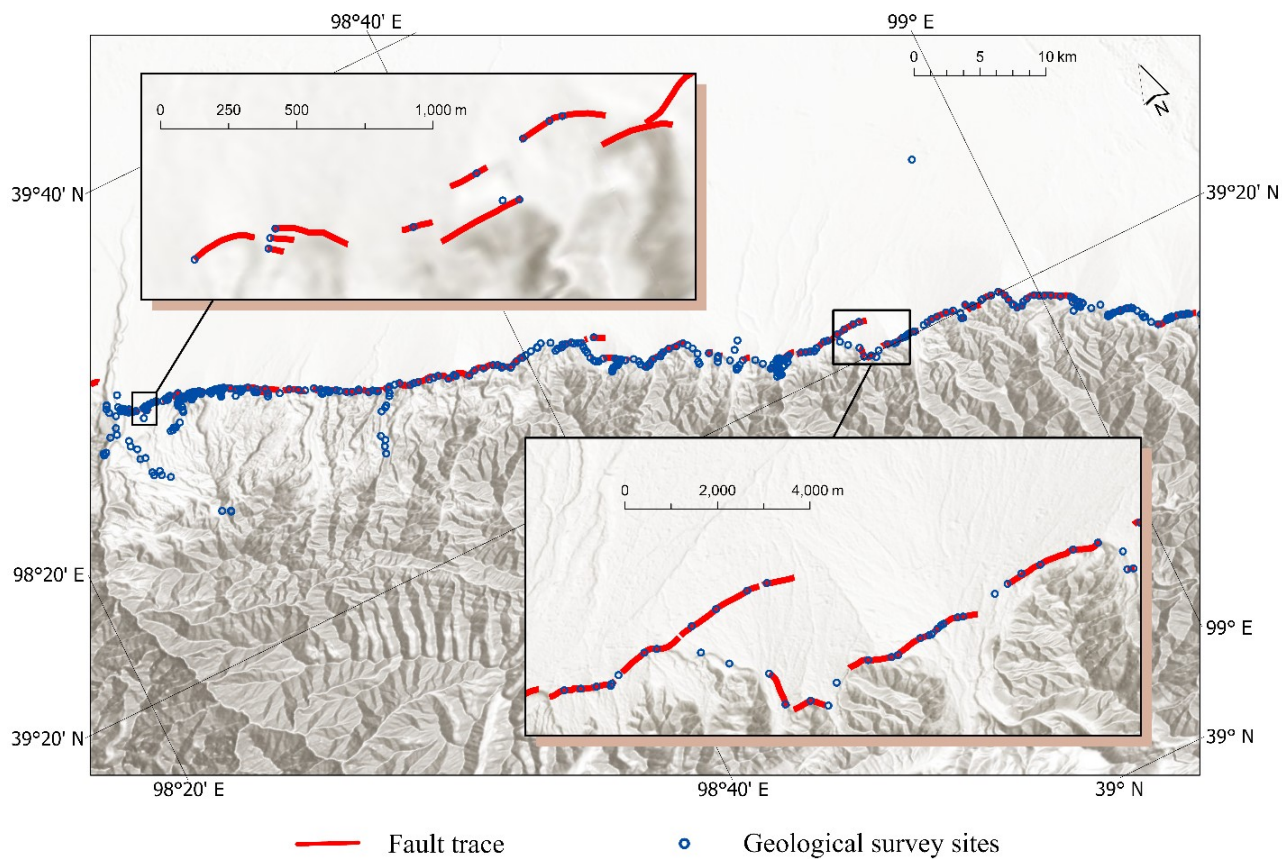
Figure 2: Survey sites for mapping of the Fodongmiao–Hongyazi Fault. The average interval of coordinate-recording sites ranges from 500–2 000 m. The fault belongs to the Qilianshan thrust fault zone at the northeastern margin of the Tibetan Plateau.
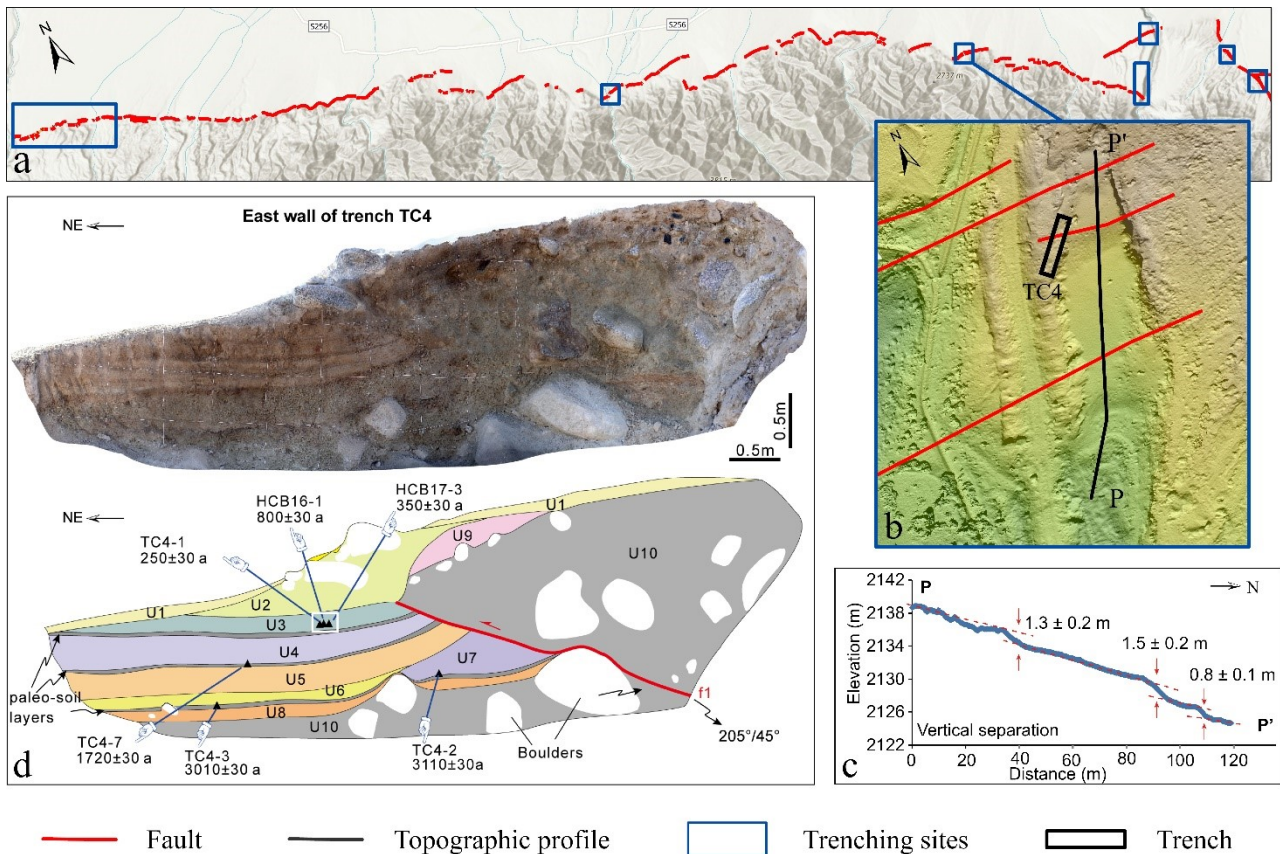
Figure 3: Key fault segment surveying example from the Fodongmiao–Hongyazi Fault (red line). (a) Distribution of the key fault segments in which geomorphic measuring, trenching, sample collecting, and paleo-earthquake trenching sites are marked by dark blue rectangles; (b) Locations of trench TC4 and topographic profile P-P′ are represented by black rectangle and black line, respectively; (c) Topographic profile (P-P′) showing fault offsets (adapted from Huang et al., 2021b); (d) Interpretation of the east wall of trench TC4 in detail (adapted from Huang et al., 2021b).

3.4 Blind fault survey method

The buried faults are those that lack near-surface exposure, potentially concealed by overlying sediments or rock formations. Firstly, we collected petroleum exploration profiles, historical earthquakes, and published literature. The location of the blind faults was inferred from the collected petroleum exploration profiles. Secondly, the historical earthquakes and published references about tectonic settings helped to figure out the faults associated with earthquakes. Thirdly, a comprehensive multi-level exploration method with geophysics and drilling sites near the collected petroleum exploration profiles was applied to determine its exact near-surface location and the position of the uppermost breakpoint of the major blind fault. Then samples obtained by drilling and dating techniques of the displaced and un-displaced strata and their dated chronological ages were used to identify their Late Quaternary activity. This method encompasses multi-level seismic exploration, joint drilling to establish fault-across geological sections, trenching, and other technologies aimed at detecting blind active faults from deep to shallow depths.

230 In this study, the blind Yinchuan active fault serves as an illustrative example (Fig. 4; Chai et al. 2006, 2011; Liu et al. 2008) to elucidate the quantitative technical requirements outlined in the Chinese mandatory standard (GB/T 36072-2018). Firstly, the seismic petroleum exploration profiles are used to reveal the approximate location of the target fault at a depth of hundreds of meters and the bottom of the Quaternary, marked by the shallowest continuous seismic reflection layer. Based on this information, a set of shallow seismic exploration profiles (in an interval of ⩽ 2.5 km) is set up on the approximate

235 ground to detect the depth of the uppermost point of the target fault. Secondly, two boreholes are drilled on both sides of the detected target fault to preliminarily verify the existence of the target faults (Fig. 5). During this exploration phase, the borehole number is gradually increased on both sides of the target fault to locate the depth of the uppermost points of the faults (Fig. 6; Chai et al., 2006; Lei et al., 2008; Wang et al., 2016). It requires at least 3 boreholes on each fault wall, with an interval of 5–45 m. The distance between the two boreholes on both sides of the target fault should be less than 10 m. Also,

240 at least one borehole is required to penetrate the bottom of the Upper Pleistocene on each side, and the final depth of other boreholes is needed to be 10 m beneath the uppermost points determined by the shallow seismic exploration (GB/T 18306-2018). The exact location and faulting age of the target blind fault could be identified by strategic analysis and sample dating of the borehole cores. If the depth of the uppermost points determined by the joint drillings is less than 10 m deep from the ground, more information on the blind fault geometry and paleo-earthquakes could be revealed by trenching. The mapped

245 blind fault trace comprises vertically projected uppermost points on the ground, obtained through the comprehensive multi-level exploration approach.
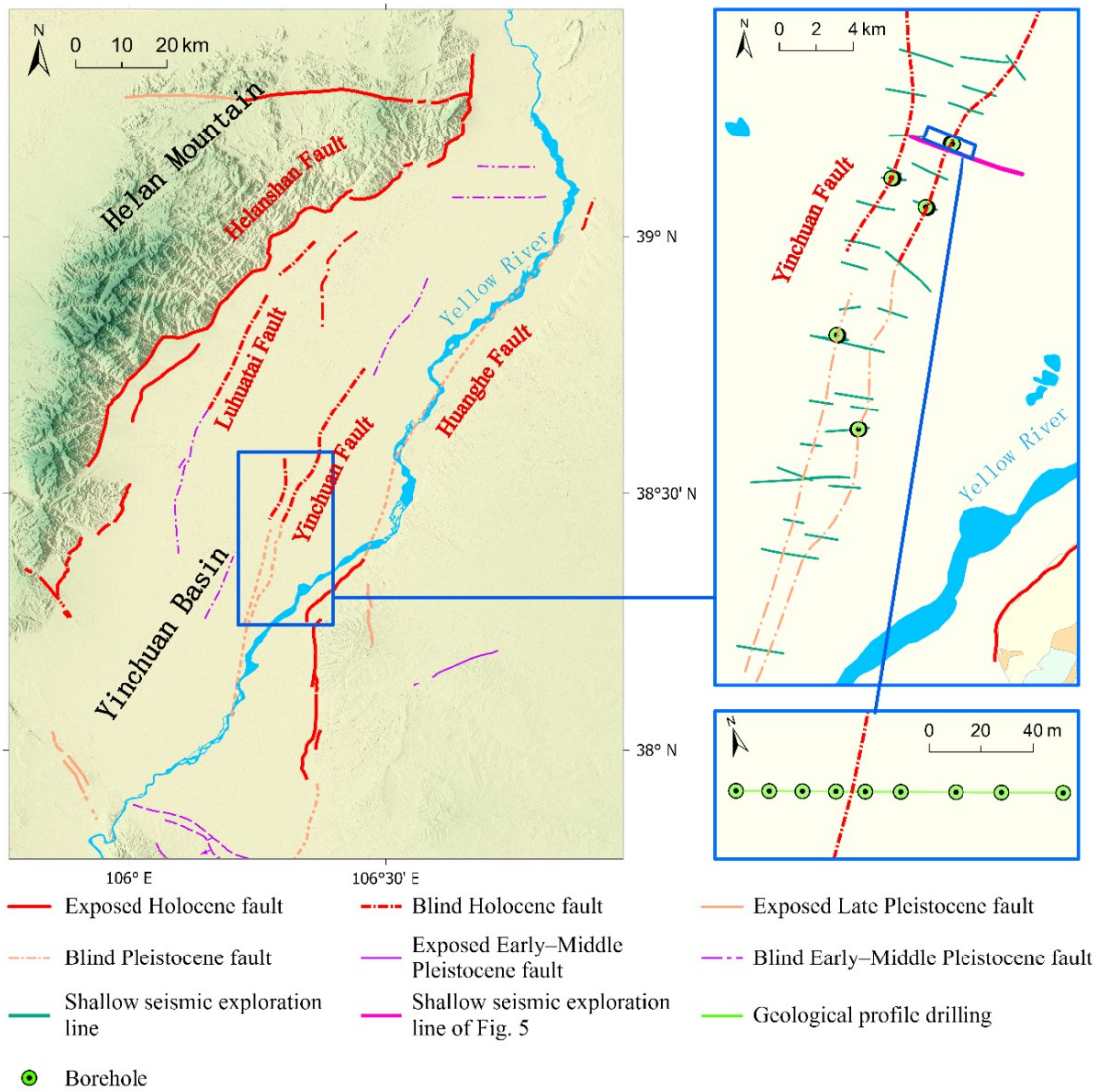
Figure 4: Map of the blind Yinchuan Fault in the Yinchuan Basin located in the northern portion of the North-South seismic zone in China.

250
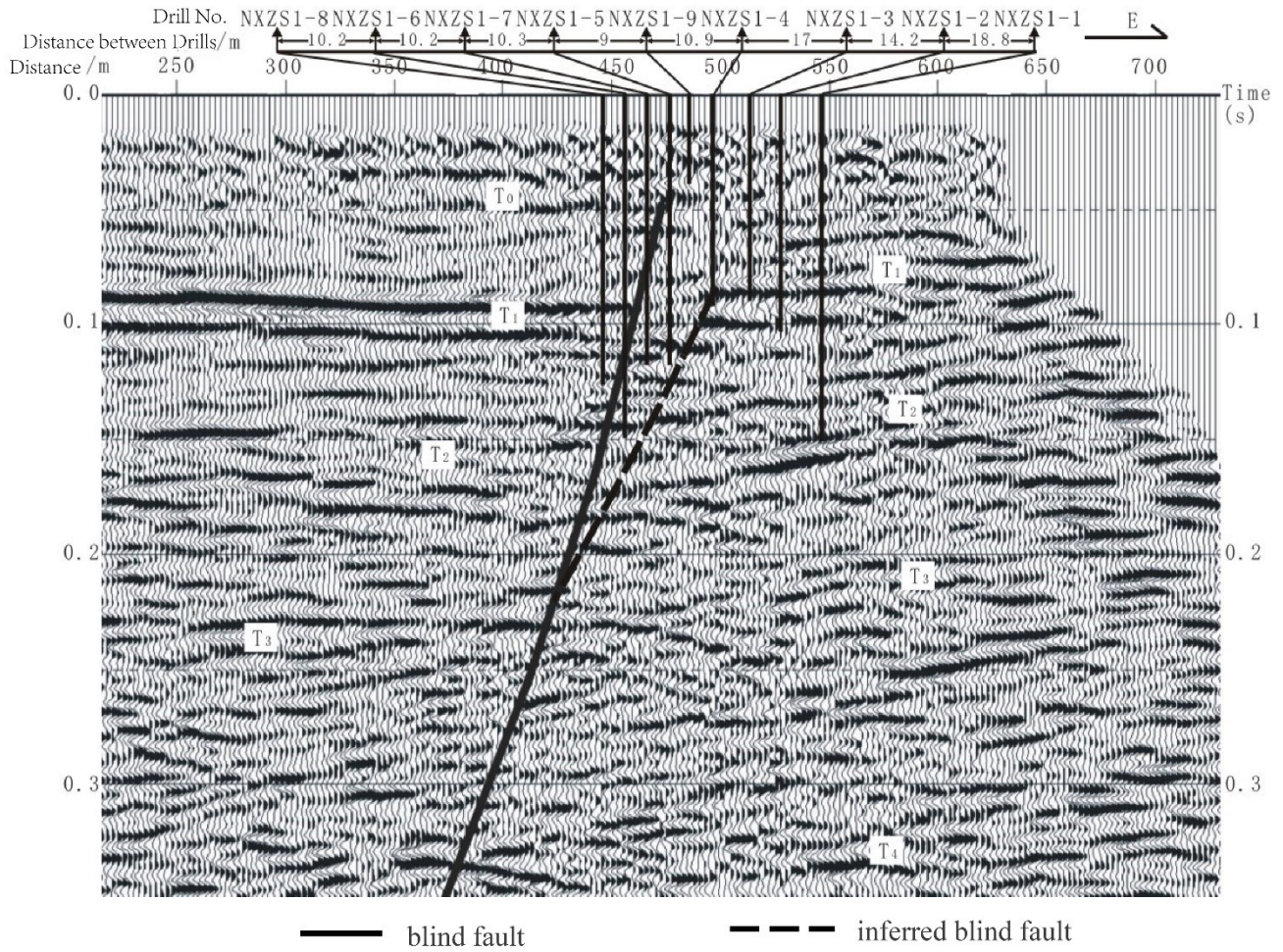
Figure 5: Approximate locations of the detected target fault and boreholes along a seismic exploration profile (adapted from Chai et al., 2011, Xu et al., 2015).
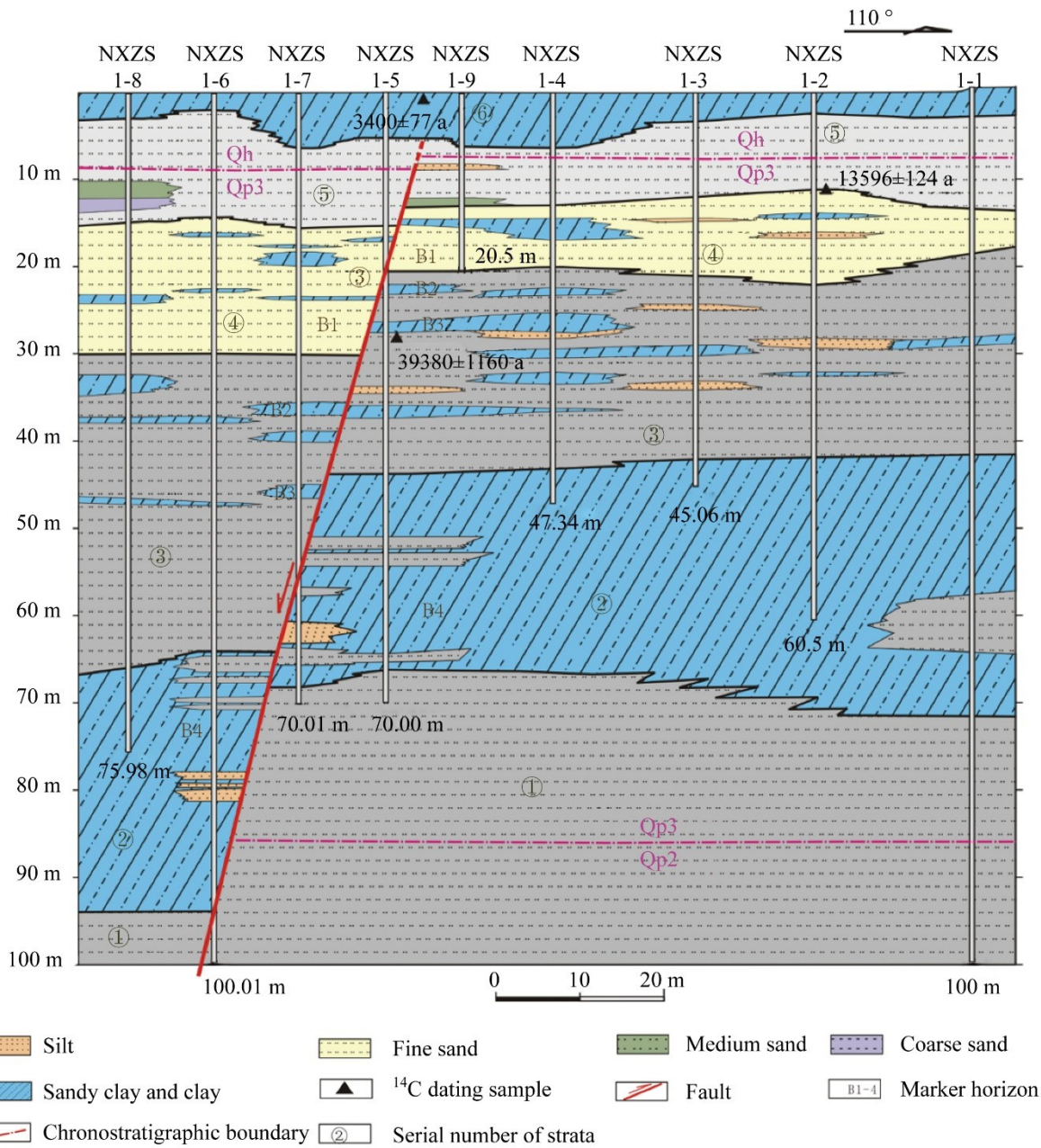
Figure 6: Joint Drilling geological cross-section at Xinqushao Village in the Yinchuan Basin (adapted from Lei et al., 2008; Chai et al., 2011).

3.5 Data sources and fundamental works

The CAFD (2023) was updated by integrating new data from the projects of active fault surveying in urban regions, seismically active fault mapping at a scale of 1:50,000 in North China and the North-South seismic zone, seismic risk assessment of active faults in key earthquake surveillance and prevention areas, and other scientific research endeavors (Fig. 7). These projects are introduced in detail below:

The projects on active fault surveying and seismic risk assessment primarily aim to identify blind or exposed seismically active faults and evaluate earthquake risk in large- and medium-sized cities, as well as in the key earthquake surveillance and prevention areas. Conversely, active fault mapping projects focus on pinpointing detailed locations of exposed seismically active faults to facilitate land-use planning and utilization (Xu et al., 2015; Zhu et al., 2005; Chai et al., 2011; Liang et al., 2013; Shen et al., 2016; Hou et al., 2012; Chen et al., 2013; Yang et al., 2010). Fundamental works within these projects encompass five main aspects: (1) identification of fault activity, (2) detection of deep faults structures within the crust, (3) assessment of earthquake risk associated with major identified faults to discern seismically active faults, (4) precise delineation of geometry for major seismically active faults, and (5) evaluation of earthquake hazards posed by seismically active faults. Achievements of these projects include mapsillustrating regional distribution of the active faults at a scale of 1:250,000 and detailed fault traces of a single active fault at a scale of 1:50,000, exploration reports, project databases, and information systems (Xu et al., 2015). All of the data obtained from the fundamental works and the project achievements are carefully reviewed by three to eight experts from a professional panel. Therefore, the data results were credible. These projects have been carried out in ~100 cities, including 26 provincial capitals and municipalities, until March 2020. Twenty urban active fault survey project databases (Table A1), which were conducted from 2002 to 2009 in Beijing, Tianjin, Shanghai, Nanjing, Ningbo, Zhengzhou, Qingdao, Hohhot, Taiyuan, Xi'an, Yinchuan, Lanzhou, Xining, Lhasa, Kunming, Urumqi, Haikou, Guangzhou, Changchun, and Shenyang (Fig. 7), are earliest fault data published and released to the public (Xu et al., 2015), and are also used to update the nationwide active fault database.

Active fault survey and mapping projects at scales of 1:50,000 and 1:250,000 received funding from the China Earthquake Administration, with the objective of acquiring precise location, spatial distribution, geometric and kinematic parameters, activity ages, slip rates, paleo-earthquake events and their recurrence intervals, and elapsed time since the last surface-rupturing event on the faults. These projects followed the procedure introduced in Sections 3.2-3.4 and meet the quantitative requirements of mandatory and recommended standards (GB/T 36072-2018; DB/T 53-2013; DB/T 65-2016; DB/T 81-2020; DB/T 82-2020; DB/T 83-2020). A professional panel reviewed the field data and mapping results. For this study, ~100 mapped faults (Fig. 7) in North China, the North-South seismic zone, and the Tien Shan region are selected to update the nationwide active fault database (Table A2).

Scientific research projects focused on addressing specific scientific inquiring concerning active faults and earthquakes. These projects delve into seismo-tectonics and seismo-genesis based on geometric and kinematic features of fault within specific sites or regions. The results provide parameters such as reliable slip rates, paleo-earthquake sequences, potential

magnitudes of future earthquakes, coseismic slips, and their distribution along the strike of seismogenic active faults. To update the nationwide active fault database in this study, data from the 2021 M 7.4 Madoi Earthquake investigation (Chen et al., 2022), 2008 M 8.0 Wenchuan Earthquake investigation (Xu et al., 2008a, 2008b, 2009a, 2009b; Chen et al., 2009), 2014 M 6.5 Ludian Earthquake investigation (Xu et al., 2014a, 2014b), Xia-Dian Fault survey (Xu et al., 2000; He et al., 2013), and research on the Tanlu Fault (Shu et al., 2016, 2020; Li et al., 2019) were utilized (Fig. 7).
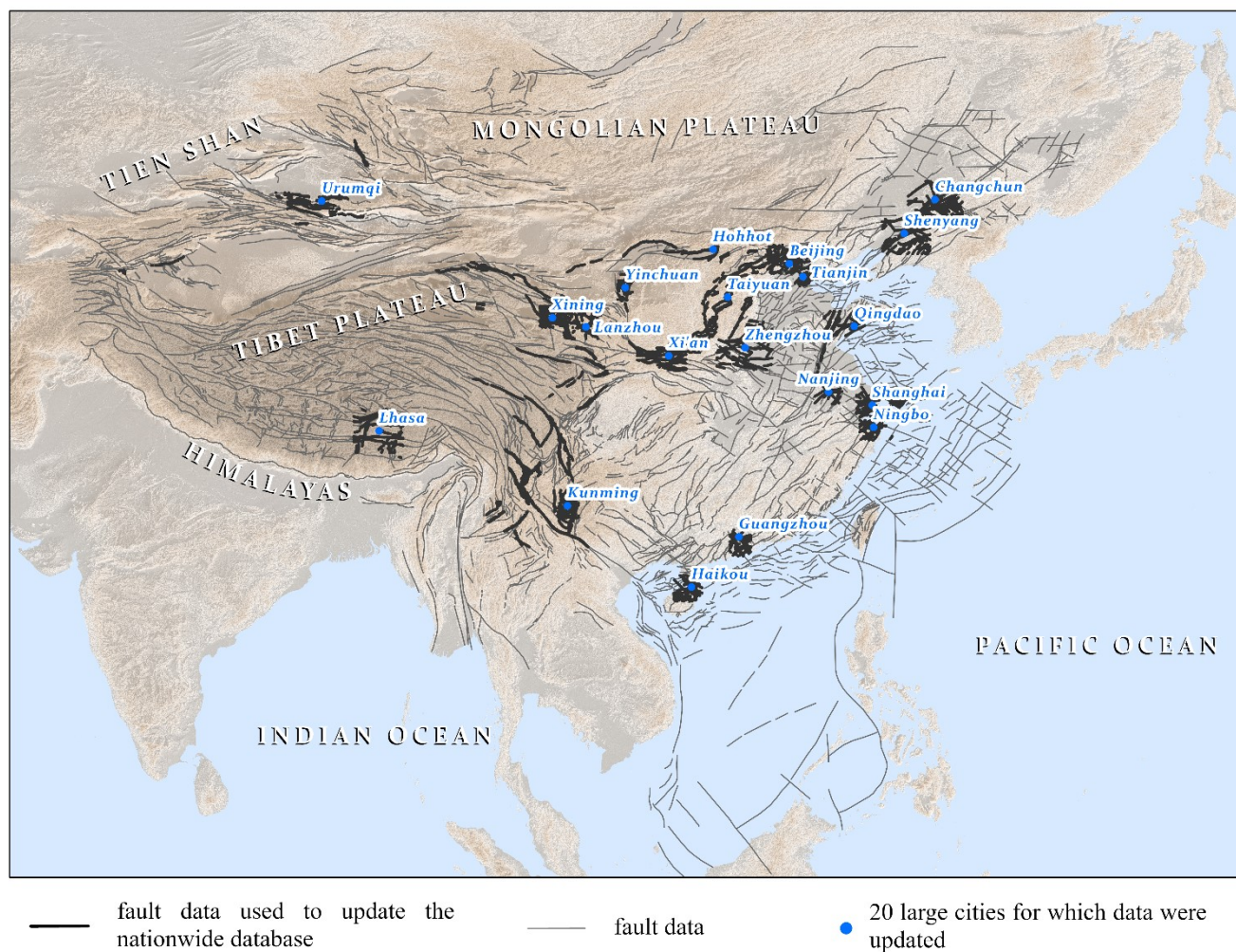
Figure 7: Sketch map of updated fault data in China.

3.6 Data processing

The CAFD (2015), along with project databases of active fault surveys and mappings in various regions, constituted a complex dataset characterized by multiple scales and varying accuracies, with a considerable total data size. As detailed in Section 1, the databases of active fault surveys and mappings comprise 100 sub-databases, totaling ~7 Terabytes of data. All

data undergo rigorous supervision and review by professional panels. For the primary objective of presenting the latest integrated achievements in this study, the individual reliability of fault data is not delineated. Instead, the individual data source of fault data is encompassed. To integrate these extensive datasets into a unified database with consistent data criteria and schema, we first integrated those project databases constructed on a regional scale and then updated the national-scale CAFD (Fig. 1). Significant updates to the 1:4,000,000 nationwide database include the refinement of activity ages and fault locations for the late Pleistocene and Holocene faults.

The project databases of active fault surveys and seismically active fault mappings are constructed by using the same criteria. They have the same data schema and use unified, well-established acquisition methods. Consequently, fault data from these two types of databases can be processed using consistent procedures, with minimal effort required for data cleaning and mining. The first step involves extracting multi-scale fault data from the 120 project databases. The second step is to integrate them. These projects are strategically planned to avoid overlap of fault data with the same scale. If the same region contains more than one fault trace, only the largest-scale data are used for integration. As the scales of the new well-mapped fault traces are equal to or even larger than 1:250,000, they are too complex to be integrated into 1:4,000,000-scale data. Therefore, the third step is to simplify the fault traces. In large-scale fault data, a fault is generally segmented for detailed investigation; hence contiguous segments may have different activity ages. One of the most important applications of the database is hardcopy or electronic image maps for earthquake emergency response (Wu, et al., 2021). The reference scale of the hardcopy maps is about 1:4,000,000~1:1,000,000. If the contiguous segments within 2 cm have different activity ages, they will be merged for map generalization. When integrated into the national scale fault data, two or even more small contiguous segments may be merged into one. Under this condition, the activity age of the merged fault trace is the same as the latest of the merged segments. For example, the blind Yinchuan fault (1:250 000) is divided into the Holocene north segment (Fig. 4a, red dotted line in the blue rectangle) and the late Pleistocene south segment (Fig. 4a, orange dotted line in the blue rectangle). The total length of those two segments is 80 km, which is only 2 cm on a 1:4,000,000 scale map. Therefore, the two segments are merged into a Holocene one.

Scientific research predominantly focuses on individual segments or a limited number of surveying sites for a given fault. These data serve to supplement the CAFD (2023), to complete and correct the national-scale fault data using a similar methodology. While the CAFD (2015) shares the same data definition and acquisition methods as previously described, its data schema slightly differs from that of project databases concerning field names and domain values. Considering that the CAFD (2015) has fewer fault traces than the project databases, we adjust the CAFD schema to fit the project databases. Subsequently, the processed data introduced in the previous two paragraphs are smoothly integrated into the CAFD (2023). The CAFD (2023) is adjusted for deployment in the Web-GIS system before being published in the last step.

3.7 Data descriptor

The active fault database undergoes translation into English prior to deployment in the system and global release, facilitating
335 access for scientists and engineers worldwide. Its fields encompass the fault zone name, fault name, fault segment name, kinematic features, and activity age (Table A3).

The fault data are graded according to size and characteristics using the fields of fault zone name, fault name, and fault segment name. A fault zone is a cluster of parallel faults such as the Tanlu and Longmenshan fault zone. In general, faults in the same fault zone exhibit congruent in geometry and kinematics, together with accumulated crustal strains, or possibly
340 connected in deep. A single-fault zone consists of single fault or several faults. A single fault is further subdivided into multiple segments based on geometry. Each segment has specific and different geometric characteristics and is a basic studied unit of a fault. Take the Fodongmiao-Hongyazi Fault (FHF) as an example (Huang et al., 2021b)(Fig. 8). It is one fault of the northern margin fault zone of the Qilianshan mountains. Its west and middle segments exhibit divergent geometric patterns: the west segment trace displays linear characteristics, while the middle segment trace resembles jagged
345 teeth. Moreover, the east segment, distinct from the middle segment, is delineated by an anticline and follows a linear trajectory. Not all faults are affiliated with a fault zone.
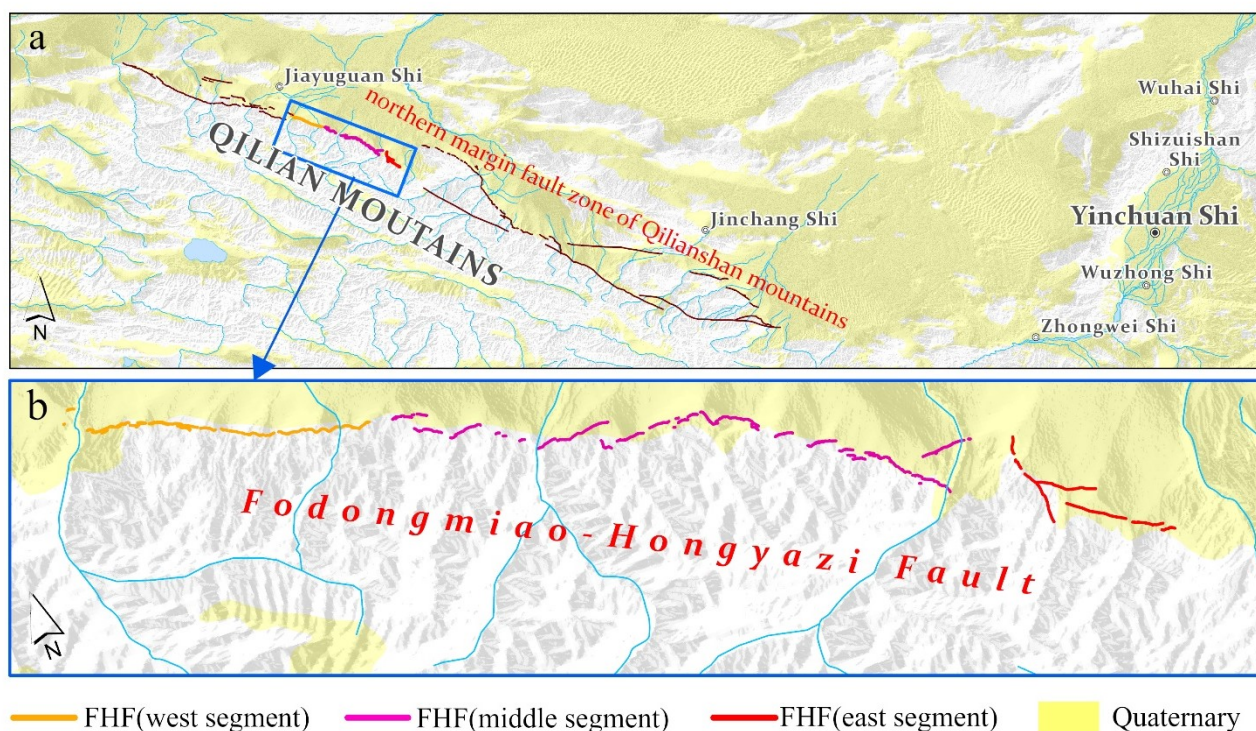
Figure 8: Map of (a) the northern fault zone of Qilianshan mountains and (b) Fodongmiao-Hongyazi Fault.

Only some important active fault line data belonging to fault zones in block boundary zones are assigned a "fault zone name". Additionally, highly scrutinized faults are segmented and the corresponding fault line data have "fault segment names." Given the intricacies and vast number of faults in China, the process of rating and naming must persist.

The field named "feature" stores information regarding the motion type and visibility of the fault on the ground. Based on the relative movement of the two walls, the faults were classified as normal, reverse, strike-slip, or oblique faults. Oblique faults consist of left- and right-oblique slip faults, with vertical components that might be either normal or reverse. Active faults are also divided into exposed and buried faults.

The active fault database is aimed at earthquake disaster prevention and focuses on the latest activity during the Quaternary. Therefore, faults are classified as the Holocene, late Pleistocene, middle–early Pleistocene and pre-Quaternary faults, denoted by the field "Age" (GB/T 36072-2018). The Holocene faults are those with active evidence from the Holocene or the past 12 000 years. For the late Pleistocene faults, active evidence exists in the late Pleistocene but not in the Holocene. The middle–early Pleistocene faults are those with the latest active evidence in the middle or early Pleistocene. For pre-Quaternary faults, active evidence is not available in the Quaternary. This means that no evidence showed that the fault displaced the Quaternary landforms or sediments. There was also no Quaternary fault age information such as the ESR dating fault gouge. Major active evidence is based on the latest dislocated stratum. This method is introduced in Sections 3.3-3.4.

3.8 Quality discussion

The CAFD (2023) collects the maximum amount of reliable data in the projects introduced in Section 3.5 launched by China Earthquake Administration, related to earthquakes with the primary objective of effectively preventing earthquake disasters by determining earthquake sources and carrying out active tectonic zonation. The spatial correlation between faults and earthquakes with magnitudes greater than 6.5 is high. The amount of fault data is large. The database contains ~7,000 fault traces,of which ~1,600 faults are named. The fault names were collected from published or unpublished papers, geological literature, or existing fault databases, utilizing two primary naming methods. One is named after the mountains and rivers. The other is named after the place name (county, village, etc.).

Active fault surveys in China are difficult because the country is located in the intersection region of the Circum-Pacific and Eurasian seismic zones, resulting in complex continental tectonics, widespread distribution of active faults, intense neotectonics and seismic activity, and inaccessible terrain. The extent of seismo-genic fault research varies from region to region. For some faults with low research extent, their geometric and kinematic parameters remain unknown or imprecise. In the periphery and interior of the Tibetan Plateau, which was formed during the collision of the Indian and Eurasian Plates, the mega-strike-slip fault systems, such as the Altyn Tagh, east Kunlun and Xianshuihe Faults, the thrust fault systems, e. g. the Himalayan frontal, the Hexi Corridor and the Longmenshan thrusts, as well as the North-South striking normal faults in the western part of the Plateau exist. The thrusts and strike-slip fault have also been developed at the northern and southern piedmonts and in its interior. In some regions in the Tien Shan (see Fig. 7) and Tibetan Plateau due to the high altitude and

snow-capped, it is difficult to carry out research work and obtain accurate fault data. Numerous oblique normal faults around the Ordos Block and strike-slip faults, such as the Tanlu fault in Eastern China exit too. Those faults are located in regions with dense urban construction and populations or thick Quaternary deposits. Therefore, it is difficult to find those fault traces on the ground and locate the blind faults underground. Besides, the spatial relationship and geometrical link of some faults, such as some segments of the Tanlu fault in Eastern China and some E-W trending faults in the Tibetan Plateau, also remain unclear.

Thus, the vector lines of such faults directly cross each other without expressing a geometrical link. In addition, research on marine and maritime island faults has been limited by surveying technology.

Given that the Active Fault Database in China is primarily based on 1:4,000,000 data but updated with 1:250,000–1:50,000 data, the overall coordinate accuracy is comparable to that of a 1:1,000,000 mapwith 1 mm representing 1 km in the real world, depicting width of the fault line symbol. The data precision is partially better than that of the 1:1 000 000 map because the reference is on a larger scale.

In conclusion, the CAFD (2023) reflects the latest research on active faults and fault data integration. More investigations of active tectonics and fault systems should be carried out in China, and the nationwide database should be updated in the future.

3.9 Application

The CAFD (2023) and its previous versions have been widely used by the Chinese government, research institutions, and associated companies. The National Geomatics Center of China and the China Petroleum & Chemical Corporation take those data as reference material for analyzing the seismotectonic environment within their information management systems. The national-scale Active Faults Database is the basic reference for compiling seismotectonic maps on both regional and national scales. Examples include the seismotectonic map of the Ordos block and its boundary zones (1:500 000; National Research and Development Program of China; No. 2017YFC150100), digital seismotectonic map of the northeastern seismic zone in China (1:1 000 000; a Spark Plan project funded by the China Earthquake Administration; No. XH18015), seismotectonic map of the Shanxi Province and its adjacent regions (1:500 000; a public service map produced by the Shanxi Earthquake Agency), and seismotectonic map of China (1:1 000 000; first comprehensive natural hazard risk investigation in China). Furthermore, these data play a crucial role in earthquake emergency response services, monitoring services, forecasting services, and earthquake disaster prevention, all under the supervision of the China Earthquake Administration. Since 2018, the database has been provided to the earthquake response departments of the China Earthquake Networks Center for emergency actions. In the same year, it was also made available to the working research group of the post-earthquake prediction technology system, a key project in earthquake monitoring and forecasting from the China Earthquake Administration (Project No. 18440680117). In 2019, this database was transferred to the China Earthquake Disaster Prevention Center to establish the Data Center for Seismic Active Fault Surveys. The Institute of Geology, China Earthquake

Administration (IG, CEA), has also produced seismotectonic maps during earthquake emergencies based on the database (Wu et al., 2021). The WFS service hosted in our system has been utilized by a commercial app (GeoQuater).

4 System Introduction

4.1 System performance and architecture

The China Earthquake and Fault Information System (CEFIS(V1), 2021), which has been available online and continuously updated since 2019, offers web services for querying earthquakes and active faults in China and adjacent regions. The CAFD (2015) has been released in the system. In 2021, the system was updated again by simplifying the interface, adding the English fields, earthquake base map, layer addition, and system sharing function. Additionally, a simplified version of a regional active fault survey map (Wu et al., 2022), introduced in Sec 3.3, is also open to the public as a map service within the additional layer list. This section provides an overview of the architecture of the current version (CEFIS (V2), 2023).

The system is built on the ArcGIS Enterprise platform 10.6 using ArcGIS Web AppBuilder in the B/S mode and is divided into four layers (Fig. 9) namely data, service, portal, and application layers.

The data layer deploys the PostgreSQL database to store active fault and earthquake data. PostgreSQL, a free open-source object-relational database system, can be connected to an ArcGIS Server deployed in the service layer. The ArcGIS Server can publish data in the form of map and feature services, which are easily accessible through web applications. The ArcGIS Portal and ArcGIS Web Adaptor are deployed in the portal layer to provide WMS and WFS services and manage user access. The ArcGIS Portal provides intuitive what-you-see-is-what-you-get applications such as AppBuilder with ready-to-use widgets, which enable the construction of map and three-dimensional scene applications on the web. The system discussed in this study is also developed using ArcGIS Web AppBuilder. Supported by these technologies, the CAFD can be accessed across various platforms including desktop software, smartphones, and online sites.
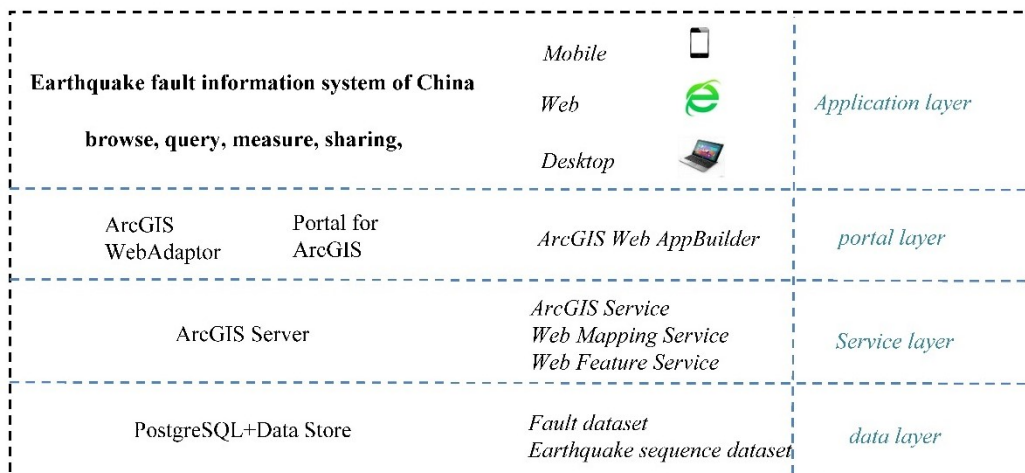
Figure 9: System architecture diagram.

4.2 Earthquake sequence data

The system uses earthquakes (M > 5.0) as a background to illustrate seismic activity on and around faults. The earthquake catalog sourced from the National Earthquake Data Center (NEDC) is converted into geographic vector data and deployed in the system (Earthquake sequence data from NEDC, 2023). This dataset encompasses historical and instrumental earthquake records preceding June 2021. The system contains three earthquake layers corresponding to the three datasets obtained from the NEDC. The NEDC provides three datasets based on specific time periods: a historical earthquake catalog (prior to ~1969.12.31.; Table A4), the earthquake catalog from the China Earthquake Networks (CEN; 1970.1.1.-2008.12.31.; Table A5), and the official earthquake catalog from the CEN (2009.1.1.-2023.7.31.; Table A6). The historic earthquake catalog compiled by Gu (1983) includes destructive earthquakes (M $\geqslant$ 5.0) that occurred from 1831 BC to 1969 AD. The CEN earthquake catalog comprises data from 88 National seismograph network stations (digital), regional someone-on-duty network stations (digital), and simulated network stations. The official earthquake catalog is from CEN, which is obtained from nationwide earthquake monitoring station networks comprising national and regional (31) station networks post-January 1, 2009.

4.3 System usage

4.3.1 System interface and function

The system is a Web Map application that displays and queries the Active Faults Database of China and its adjacent regions. It is publicly available worldwide. Its interface comprises seven components (Fig. 10): (a) web map, (b) eagle-eye map, (c) attribute table, (d) browsing tools, (e) address geolocation tool, and (f & g) system tools.

The language of the system interface is determined by the browser's default settings. The data field values are presented in both English and Simplified Chinese within the attribute table and Query dialogue. Thus, the system can be used by both English and Chinese-speaking users. Additionally, users proficient in languages such as French, German, Russiancan also use the system.
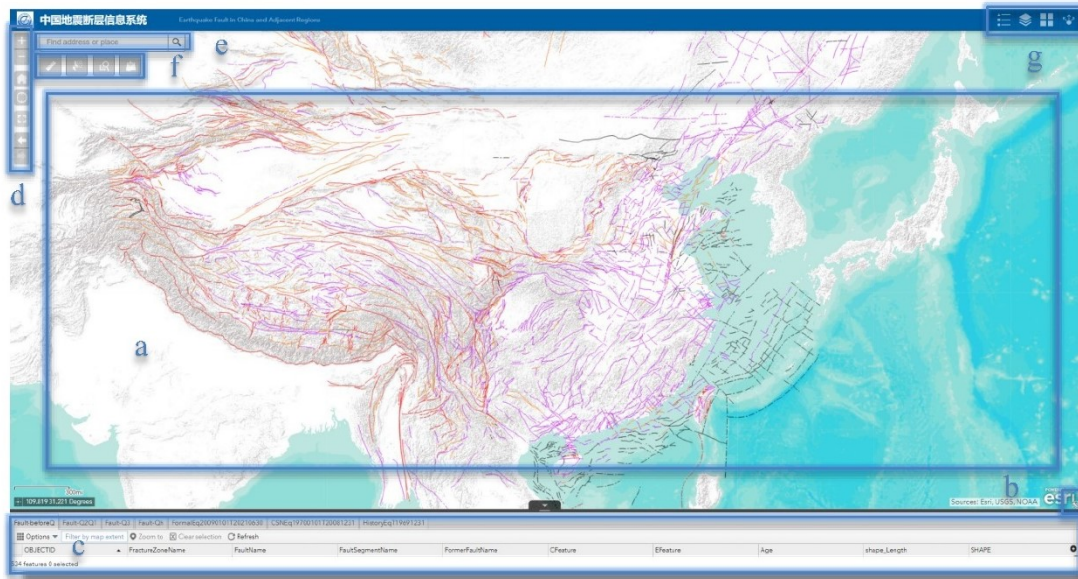
460 **Figure 10: System interface. (a) Web map displaying only fault traces in full extent view; when zoomed into the regional scale, earthquake epicenters will appear on the map. (b) Accordion overview map. (c) Accordion attribute table. (d) Navigation toolbar; the tools from top to bottom are zoom in, zoom out, default extent, zoom to the current position, full extent, previous view, and next view. (e) Address geolocation tool. System tools: (f) measurement, selection, inquiry, and layer addition (from left to right) and (g) legend, layer controller, base maps, and sharing (from left to right).**

465 **4.3.2 Data query and export**

The system offers four methods for querying fault information: (1) The menu within the attribute table window (Fig. 10a) provides a "filter" tool to query faults with certain conditions (Fig. 11a); (2) the second tool is a spatial selection tool (Fig. 10f) for fault and earthquake data (Fig. 11c); (3) the third tool allows fault queries by feature, activity age, or name under specific spatial conditions (Figs. 11b and 10f); (4) the address geolocation tool (Fig. 10e) can be used to zoom the map into a

470 specific region and export the faults in that region (Fig. 11d). The system supports exporting query results through various methods (Fig. 11).
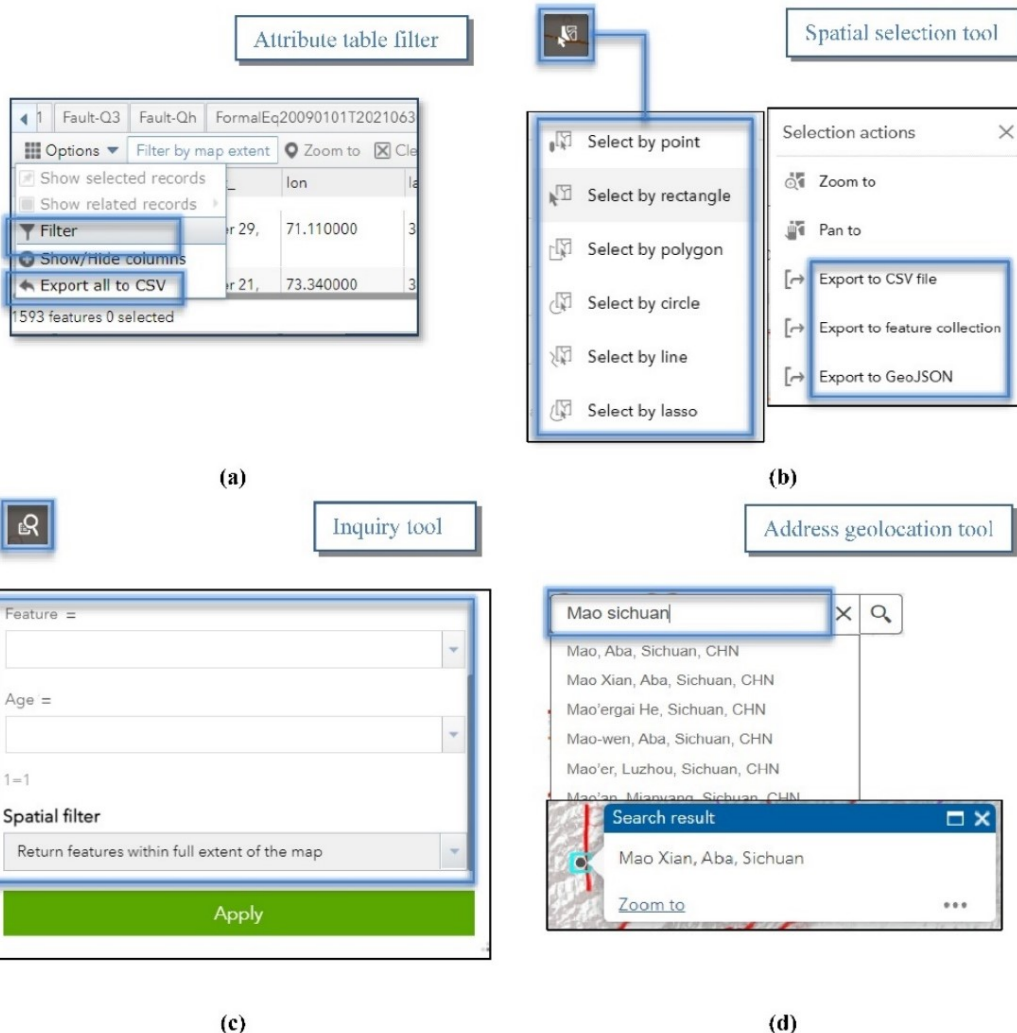
Figure 11: Data query and export tools: (a) attribute table filter, (b) spatial selection tool, (c) inquiry tool, and (d) address geolocation tool (translated by Google Chrome).

4.4 How to use the data service

The system publishes the Open Geospatial Consortium (OGC) WFS and WMS of the active fault database of China. The OGC WFS and WMS are dynamic services that offer realtime maps on the web, adhering to OGC specifications. These services facilitate open and authentic access to web maps across different platforms and clients. Available operations of the WMS in the system in this study are GetCapabilities, GetLegendGraphic, GetSchemaExtension, GetFeatureInfo, and GetMapGetStyles. Compared with WMS, WFS provides greater data access, benefiting from its ability to insert, update, delete, retrieve, and discover geographic elements over HTTP in a distributed environment. The available WFS operations encompass GetCapabilities, DescribeFeatureType, GetPropertyValue, GetFeature, GetGmlObject, ListStoredQueries, and

DescribeStoredQueries. In esence, data can be browsed, queried, analyzed, and downloaded from the system, but not revised.
Furthermore, fault layers can be integrated into GIS software for analysis through WMS and WFS, such as ArcGIS Pro and QGIS (Fig. 12).
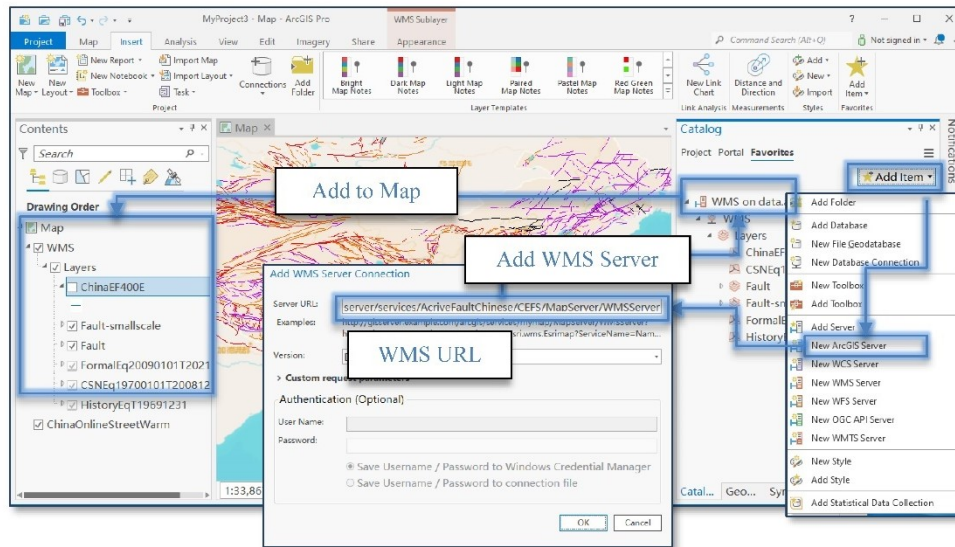
(a)
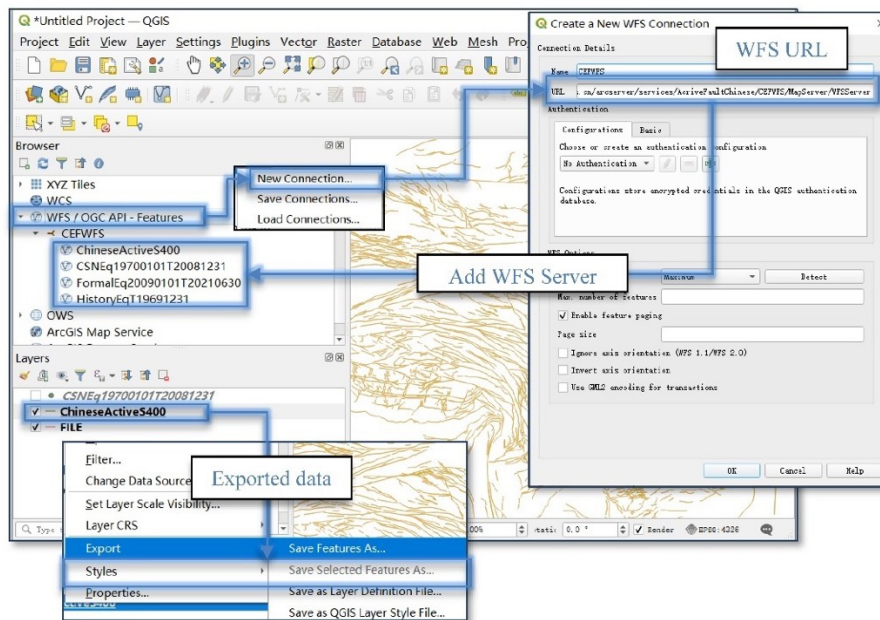
(b)

Figure 12: (a) How to add WMS Server in ArcGIS Pro. (b) How to add WFS Server in QGIS and export data.

5 Conclusions

The CAFD (2023) integrates both the national-scale fault database and the latest decadal regional-scale fault survey data. The database, along with its previous versions. have been widely applied in government departments, research institutes, and commercial companies. China is situated in the intersection between the Circum-Pacific and Eurasian seismic zones with numerous complex continental tectonics, active faults, and earthquake activity. However, challenges persist in surveying or locating active faults in certain regions due to inaccessible terrain and anthropogenic activities. Active faults should be considered for earthquake disaster mitigation. Therefore, the database will be gradually updated in the future based on future references, and a later version may be released on the system if it is finished.

The first version of the web system (CEFIS (V1), 2021) has performed effectively for nearly 2 years and its second version (CEFIS (V2), 2023) was released in 2021 and has also been operating well. This study delineates the architecture, interface, function, and usage of the system, serving as a platform for querying and analyzing the integrated active faults database in China., This database encapsulates crucial information pertaining the location, latest activity age, and kinematic characteristics of the faults. The system can be used by both English and Chinese-speaking users. Additionally, users proficient in languages such as French, German, Russiancan also use the system.

Data and services are openly shared worldwide via the web system. The data can be downloaded from a browser or GIS software. A third-party application can link to and use the WMS and WFS services (CAFD WMS, 2023; CAFD WFS, 2023). Users can get help from the ArcGIS online document. Section 4.4 lists the available operations of the services.

6 Data availability

The CAFD and web system are accessible at CEFS (V2) under the DOI:

https://doi.org/10.12031/activefault.china.400.2022.db (Xu, 2022). The WMS (CAFD WMS, 2023) and WFS (CAFD WFS, 2023) services of the active fault are accessible online. The data are downloadable through diverse platforms and clients as introduced in Sections 4.3.2 and 4.4. The Earthquake catalogs are downloaded from the Data Sharing Infrastructure of the National Earthquake Data Center (http://data.earthquake.cn) The data are not freely downloadable. Their information and links are below.

FormalEq20090101T20230630 (Fig. 13):

https://data.earthquake.cn/datashare/report.shtml?PAGEID=datasourcelist&dt=40280d0453e414e40153e44861dd0003

515 Figure 13: the translated English websites for FormalEq20090101T20210630.

CSNEq19700101T20081231 (Fig. 14):

https://data.earthquake.cn/datashare/report.shtml?PAGEID=datasourcelist&dt=40280d0453e414e40153e44861dd0002

Figure 14: the translated English websites for CSNEq19700101T20081231.

HistoryEqT19691231 (Fig. 15):

https://data.earthquake.cn/datashare/report.shtml?PAGEID=datasourcelist&dt=8a85efd754e7d6910154e7d691810000

⬇ Download online

| 📙 updated on 2016-12-12 | 🗂 5136 pieces of data | 🕐 58,515 data visits | ⭐ Data sharing methods are available for online download |

Basic information about the data

Data Name:	Catalogue of Historical Earthquakes in China
Classification	Historical seismic data (D34000)
Spatial Scope:	nationwide
Time Frame:	1831 BC to 1969 AD
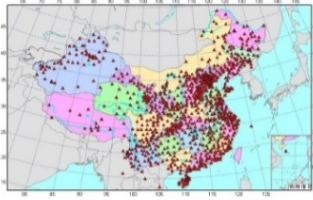
Data contact information

Contact: Mr. Li

Telephone: 8911325676

E-mail: datashare@seis.ac.cn

Unit: China Earthquake Network Center

Data summary

The catalogue was edited by Gu Gongxu, and collected the destructive earthquakes that occurred in China between 1831 BC and 1969 AD (M>=4.0), with a total of 5163 catalogues.

Instructions for data use

The reference refers to the following specifications: Chinese published results: The data are from the National Earthquake Science Data Center (http://data.earthquake.cn) of the China Earthquake Network Center. Data Sharing Infrastructure of National Earthquake Data Center (http://data.earthquake.cn). Acknowledgments can be made in accordance with the following guidelines: Chinese acknowledgment: "Thanks to the China Earthquake Network Center and the National Earthquake Science Data Center (http://data.earthquake.cn) for providing data support. Acknowledgement for the data support from " China Earthquake Networks Center, National Earthquake Data Center. (http://data.earthquake.cn)".

Detailed description of the data Data citation method

The catalogue was edited by Gu Gongxu, and collected the destructive earthquakes that occurred in China between 1831 BC and 1969 AD (M>=4.0), with a total of 5163 catalogues.

Data source

National Seismological Data Center (http://data.earthquake.cn/)

Methods of data generation or processing

Data quality description

Figure 15: the translated English websites for HistoryEqT19691231.

525

530

7 Appendix A

Table A1: Cities list for updating the CAFD

No.	City Name	Work Content	Reference Scale
1	Beijing	UAFS	1:250000
2	Haikou	UAFS	1:250000
3	Hohhot	UAFS	1:250000
4	Kunming	UAFS	1:250000
5	Lhasa	UAFS	1:250000
6	Nanjing	UAFS	1:250000
7	Ningbo	UAFS	1:250000
8	Qingdao	UAFS	1:250000
9	Shanghai	UAFS	1:250000
10	Shenyang	UAFS	1:250000
11	Taiyuan	UAFS	1:250000
12	Xian	UAFS	1:250000
13	Changchun	UAFS	1:250000
14	Zhengzhou	UAFS	1:250000
15	Urumqi	UAFS	1:250000
16	Xining	UAFS	1:250000
17	Guangzhou	UAFS	1:250000
18	Tianjin	UAFS	1:250000
19	Lanzhou	UAFS	1:250000
20	Yinchuan	UAFS	1:250000
	UAFS: Urban Active Fault Survey		

535 **Table A2: Faults list for updating the CAFD**

No.	Project Name (Named by the Fault Name)	Work Content	Reference Scale
1	Altyn Tagh fault (Eastern segment)	SM	1:50000
2	Anninghe fault (Middle segment)	SM	1:50000
3	Anninghe fault (Northern segment)	SM	1:50000
4	Anninghe fault (Southern segment)	SM	1:50000
5	Anqiu-Juxian fault	SM	1:50000
6	Bailongjiang fault	SM	1:50000
7	Bayinhaote fault zone	SM	1:250000
8	Bodongmiao-Hongyazi fault	SM	1:50000
9	Cangma fault	SM	1:50000
10	Chenghai fault	SM	1:50000
11	Cixian-Daming fault	SM	1:50000

12	Daju fault	SM	1:50000
13	Daliangshan fault	SM	1:50000
14	Daqingshan piedmont fault	SM	1:50000
15	Dayingjiang fault	SM	1:50000
16	Deqin-Zhongdian fault	SM	1:50000
17	earthen foothill fault of the Helanshan mountains	SM	1:50000
18	Eastern foothill fault of the Liupanshan mountains	SM	1:50000
19	Eastern foothill fault of the Luoshan mountains	SM	1:50000
20	eastern foothill fault of the Yulongxueshan Mountains	SM	1:50000
21	eastern foothill fault of the Yumushan Mountains	SM	1:50000
22	Fukangnan fault	SM	1:50000
23	Ganzi-Yushu fault	SM	1:50000
24	Guanggaishan-Dieshan fault	SM	1:50000
25	Guanguanling fault	SM	1:50000
26	Guguan-Baoji fault	SM	1:50000
27	Haixiu fault	IFA	1:250000
28	Hanan-Qingshanwan-Mobali fault	SM	1:50000
29	Hanmuba-Lancang fault and Hanmuba fault	SM	1:50000
30	Hanxia-Dahuanggou fault	SM	1:50000
31	Heqing-Eryuan fault	SM	1:50000
32	Heyang-Hancheng fault	SM	1:50000
33	Honghe fault (Northern segment)	SM	1:50000
34	Honghe fault (Middle segment)	SM	1:50000
35	Honghe fault (Southern segment)	SM	1:50000
36	Huashan piedmont fault	SM	1:50000
37	Huoshan fault	SM	1:50000
38	Jiaocheng fault zone	SM	1:50000
39	Jinshajiang fault	IFA	1:250000
40	Jintananshan fault	SM	1:50000
41	Junggar Basin south margin fault and Huoerguosi-Manasi-Tugulu fault	SM	1:50000
42	Keketuohai-ertai fault	SM	1:50000
43	Keping fault	SM	1:50000
44	Kusaihu-Maqu fault and Maqu-Heye fault	SM	1:50000
45	Langshan piedmont fault (Eastern segment)	SM	1:50000
46	Langshan piedmont fault (Western segment) and Sertengshan Piedmont fault	SM	1:50000
47	Laohushan fault and Maomaoshan fault	SM	1:50000
48	Lenglongling fault	SM	1:50000

49	Lijiang-Xiaojinhe fault	SM	1:50000
50	Lintan-Dangchang fault	SM	1:50000
51	Litang fault & Dewu fault & Labo fault & Xisasi fault	SM	1:50000
52	Litan-Yidun fault	SM	1:50000
53	Liulengshan piedmont fault	SM	1:50000
54	Longlin-Ruili fault	SM	1:50000
55	Longmenshan fault Zone (Middle segment)	SM	1:50000
56	Longpan-Qiaohou fault	SM	1:50000
57	Longriba fault	SM	1:50000
58	Luoyunshan piedmont fault	SM	1:50000
59	Minjiang fault and Huya fault	IFA	1:50000
60	Minle-Damaying fault	SM	1:50000
61	Nantinghe fault	SM	1:50000
62	Ninglang fault	SM	1:50000
63	North margin fault of the Xuanhua Basin and Southern margin fault of the Shenjin basin	SM	1:50000
64	northern foothill fault of the Hengshan mountains	SM	1:50000
65	Northern margin fault of Emeitaidi	SM	1:50000
66	Northern margin fault of Huaian basin	SM	1:50000
67	Northern margin fault of the Daihai	SM	1:50000
68	Northern margin fault of the Ordos Basin (Western segment)	IFA	1:250000
69	Qujiang fault	SM	1:50000
70	Riyuanshan fault	SM	1:50000
71	Sanweishan fault	SM	1:50000
72	Sertengshan Piedmont fault	SM	1:50000
73	Shiping-Jianshui fault	SM	1:50000
74	Southern margin fault of Huaian basin	SM	1:50000
75	Southern margin fault of the Balikun Basin	SM	1:50000
76	Southern margin fault of the Chaiwobao Basin	SM	1:50000
77	Southern margin fault of the Wuwei Basin	SM	1:50000
78	Southern margin fault zone of the Yuguang Basin	SM	1:50000
79	Taibai-Weishan piedmont fault	SM	1:50000
80	Taigu fault	SM	1:50000
81	Tanlu fault zone	SM	1:50000
82	Tazang fault	SM	1:50000
83	TianqiaoGou-Huangyangchuan fault	SM	1:50000
84	Tomloan fault & Kazikeaerte fault	SM	1:50000
85	Weixi-Qiaohou-Weishan fault	SM	1:50000

86	Wulashan piedmont fault	SM	1:50000
87	Xiadian fault	SM	1:50000
88	Xiangshan-Tianjingshan fault	SM	1:50000
89	Xianshuihe fault (Northern & Middle segment)	SM	1:50000
90	Xianshuihe fault (Moxi segment/Southern segment)	SM	1:50000
91	Xiaojiang fault (Middle segment)	SM	1:50000
92	Xiaojiang fault (Northern segment)	SM	1:50000
93	Xiaojiang fault (Southern segment)	SM	1:50000
94	Yabulai fault	SM	1:50000
95	Yemahe Snow Mountain Fault Zone	SM	1:50000
96	Yuanmou fault	SM	1:50000
97	Yumen fault	SM	1:50000
98	Yunongxi (Bawolong) fault	SM	1:50000
99	Zemuhe fault	SM	1:50000
100	Zhongtiaoshan piedmont fault	SM	1:50000

SM: survey mapping. IFA: identification of fault activity.

Table A3: Attributes of fault data.

Field name	Description
FractureZoneName_Ch	(in simplified Chinese) Fracture zone name. Only some
FractureZoneName_En	(in English) Fracture zone name.
FaultName_Ch	(in simplified Chinese) Fault name.
FaultName_En	(in English) Fault name.
FaultSegmentName_Ch	(in simplified Chinese) Fault segment name.
FaultSegmentName_En	(in English) Fault segment name.
FormerFaultName	(in simplified Chinese) Former name of fault.
Feature_Ch	(in simplified Chinese) Kinetic property and detectability of the fault segment.
Feature_En	(in English) Kinetic property and detectability of the fault segment.
Age	(in English abbreviations) The active age of the fault segment.

540

Table A4: Attributes of HistoryEqT19691231.

Field Name	Description
time_beiji	The origin date and origin time of the earthquake (GMT +8).
lon	Epicentral longitude of the earthquake.
lat	Epicentral latitude of the earthquake.

Field Name	Description
dep	The focal depth of the earthquake is in km.
magnitude	Magnitude (M).
intensity	(Macro) epicentral intensity.

Table A5: Attributes of CSNEq19700101T20081231.

Field Name	Description
time_gmt_	The origin date and origin time of the earthquake (GMT).
lon	Epicentral longitude of the earthquake.
lat	Epicentral latitude of the earthquake.
dep_km_	The focal depth of the earthquake is in km.
ms	Surface wave magnitude.
ms7	Surface wave magnitude was computed from records of the Chinese-made long-period seismograph of type 763 (Cheng et al., 2017).
ml	Local magnitude.
mb	Body wave magnitude, measured by short-period body wave recording (mb).
mb_1	Body wave magnitude, measured by medium-period body wave recording (mB).

545 **Table A6: Attributes of FormalEq20090101T20230730.**

Field Name	Description
Date	The origin date and origin time of the earthquake (GMT +8).
lon	Epicentral longitude of the earthquake.
lat	Epicentral latitude of the earthquake.
dep_km_	The focal depth of the earthquake in km.
magnitudet	Magnitude type.
magnitude	Magnitude.

Author contributions

Conceptualization, XX, and XW; Data curation, GY, XW, GC, JR, KL, and CX; Formal analysis, KD, XX, XW, GY; Funding acquisition, XX, GY, and XW; Investigation, XX, XW, GY, GC, XY, HY, and XH; Methodology, GY, XW, KD, 550 GC, JR, KL, and CX; Project administration, XX, GY, and XW; Software, KD and XW; Supervision, XX and GY; Validation, XX and XW; Writing, XW and XX. All authors have read and agreed to the published version of the manuscript.

Competing interests

The authors declare that they have no conflict of interest.

Acknowledgments

555 We acknowledge all colleagues who have contributed to the active fault databases in China in the past decades. Many scientists and engineers have participated in active fault surveys and mappings and made efforts to build regional-scale project databases. Their work provided basic high-quality materials.

The Earthquake catalogs are downloaded from the Data Sharing Infrastructure of the National Earthquake Data Center (http://data.earthquake.cn). We acknowledge the data support from the "China Earthquake Networks Center, National Earthquake Data Center."

Financial support

This research work was supported by the National Natural Science Foundation of China (Grant No. 41941016) and the

Research and Development Program of IG, CEA (Name: active fault data management on a cloud platform).

References

Basili R., Valensise G., Vannoli P., Burrato, P., Fracassi, U., Mariano, S., Tiberti, M. M., and Boschi, E.: The Database of Individual Seismogenic Sources (DISS), version 3: summarizing 20 years of research on Italy's earthquake geology, Tectonophysics, 453(1-4), 20-43, https://doi.org/10.1016/j.tecto.2007.04.014, 2008.

Basili R., Burrato P., De Santis G. M., Fracassi, U., Maesano, F. E., Tarabusi, G., and DISS Working Group.: Database of Individual Seismogenic Sources (DISS), Version 3.3. 0: A compilation of potential sources for earthquakes larger than M 5.5 in Italy and surrounding areas, https://doi.org/10.13127/diss3.3.0, 2021.

CEFIS (V1): http://www.neotectonics.cn/arcgis/apps/webappviewer/index.html?id=3c0d8234c1dc43eaa0bec3ea03bb00bc, last access: 27 Nov 2021.

CEFIS (V2): https://data.activetectonics.cn/arcportal/apps/webappviewer/index.html?id=684737e8849c4170bbca14447608c451, last access: 12 May 2023.

CAFD WFS: http://data.activetectonics.cn/arcserver/services/Hosted/CAFD400_2022_WFS/MapServer/WFSServer, last access: 12 May 2023.

CAFD WMS: https://data.activetectonics.cn/arcserver/services/AcriveFaultChinese/CEFSL_CE/MapServer/WMSServer, last access: 12 May 2023.

Chai, C., Meng, G., Du, P., Wang, Y., Liu, B., Shen, W., Lei, Q., Liao, H., Zhao, C., Fan, S., Zhang, X., and Xie, X.: Comprehensive multi-level exploration of buried active fault: an example of Yinchuan buried active fault, Seismology and Geology, 28(4), 536, 2006 (in Chinese).

Chen, G., Xu, X., Yu, G., An, Y., Yuan, R., Guo, T., Gao, X., Yang, H. and Tan, X.: Co-seismic slip and slip partitioning of multi-faults during the MS8.0 2008 Wenchuan earthquake, Chinese J. Geophys.-Ch., 52(5), 1384-1394, https://doi.org/10.3969/j.issn.0001-5733.2009.05.028, 2009.

Chai, C., Meng, G. and Ma, G.: Active fault survey and earthquake hazard assessment in Yinchuan, Science Press, ISBN 978-7-03-030701-9, 2011 (in Chinese).

Chen, Y.: Active fault survey and earthquake hazard assessment in Tianjin, Science Press, ISBN 978-7-03-037079-2, 2013.

Chen, G., Xu, X., Wen, X., and Chen, Y.: Late Quaternary Slip-rates and Slip Partitioning on the Southeastern Xianshuihe Fault System, Eastern Tibetan Plateau, Acta Geol. Sin.-Engl., 90(2), 537-554, https://doi.org/10.1111/1755-6724.12689, 2016.

Chen, J., Rong, Y., Harold, M., Chen, G., and Xu, X.: An Mw-Based Historical Earthquake Catalog for Mainland China, B. Seismol. Soc. Am., 107(5), 2490–2500, https://doi.org/10.1785/0120170102, 2017.

595 Chen, G., Li, Z., Xu X., Sun, H., Ha, G., Guo, P., Su, P., Yuan Z., Li, T.: Co-seismic surface deformation and Late Quaternary accumulated displacement along the seismogenic fault of the 2021 Madoi M7.4 earthquake and their implications for regional tectonics, Chinese Journal of Geophysics, 65(8): 2984-3005, https://doi.org/10.6038/cjg2022P0873, 2022 (in Chinese).

DB/T 53-2013 Mapping of active fault in 1:50 000, recommended standard by China Earthquake Administration, 2013 (in 600 Chinese).

DB/T 65-2016 Code of 1:50 000 active fault mapping database, recommended standard by China Earthquake Administration, 2016 (in Chinese).

DB/T 81-2020 Active fault survey-Paleoseismic trenching, recommended standard by China Earthquake Administration, 2020 (in Chinese).

605 DB/T 82-2020 Active fault survey-Field geological investigation, recommended standard by China Earthquake Administration, 2020 (in Chinese).

DB/T 83-2020 Active fault survey-Inspection of database, recommended standard by China Earthquake Administration, 2020 (in Chinese).

Deng, Q., Lu, Z., Yang, Z.,: Remarks on urban active faults exploration and associated activity assessment. Seismology and 610 Geology, 29(2): 189-200, 2007 (in Chinese).

Deng, Q., Zhang, P., Ran, Y., Yang, X., Min, W., and Chu, Q.: Basic characteristics of active tectonics in China, Sci. China Ser. D., 32(1), 1020-1030, https://doi.org/10.1360/zd2002-32-12-1020, 2002 (in Chinese).

Deng, Q., Zhang, P., Ran, Y., Yang, X., Min, W., and Chu, Q.: Basic characteristics of active tectonics of China, Sci. China Ser. D., 46(4), 356-372, https://doi.org/10.1360/03yd9032, 2003 (in Chinese).

615 Deng, Q., Ran, Y., Yang, X., Min, W., and Chu, Q.: The active tectonic map of China (1:4 000 000), Seismological Press, ISBN 978-7-50-283051-9, 2007 (in Chinese).

Emre, Ö., Duman, T. Y., Özalp, S., Şaroğlu, F., Olgun, Ş., Elmacı, H., and Çan, T.: Active fault database of Turkey. B. Earthq. Eng., 16(8), 3229-3275, https://doi.org/10.1007/s10518-016-0041-2, 2018.

Earthquake sequence data from NEDC: https://data.earthquake.cn/gcywfl/index.html, last access: 20 Jan 2023.

620 GB/T 18306-2015 Seismic ground motion parameters zonation map of China, mandatory standard of China, 2015 (in Chinese).

GB/T 33177-2016 National fundamental scale maps—1:5 000 1:10 000 topographic maps, 2016 (in Chinese).

GB/T 33178-2016 National fundamental scale maps 1:250 000 1:500 000 1:1 000 000 orthophoto maps, 2016 (in Chinese).

GB/T 36072-2018 Surveying and prospecting of active fault, mandatory standard of China, 2018 (in Chinese).Ganas A., 625 Oikonomou I. A., and Tsimi C.: NOAfaults: A digital database for active faults in Greece. B. Geol. Soc. Greece, 47(2), 518-530, 2013.

GB18306: http://www.gb18306.net/detail/50, last access: 20 Jan 2023.

Geology Institute of China Earthquake Administration (GICEA), Seismotectonic map of China (1:4 000 000), 1979 (in Chinese).

630   Gu, G.: Earthquake catalogue of China (from 1831 BC to 1969 AD), Science Press, ISBN 13031·2238, 1983 (in Chinese).

Guo P., Han Z., Dong S., Mao, Z., Hu, N., Gao, F., and Li, J.: Latest quaternary active faulting and paleoearthquakes on the southern segment of the Xiaojiang fault zone, SE Tibetan plateau, Lithosphere, 2021(1), https://doi.org/10.2113/2021/7866379, 2021.

Haller, K. M., Machette, M. N., Dart, R. L., and Rhea, B. S.: U.S. Quaternary fault and fold database released, Eos, 635   Transactions American Geophysical Union85(22), 218-218, https://doi.org/10.1029/2004EO220004, 2004.

Hou, K.: Active fault survey and earthquake hazard assessment in Nanjing, Seismological Press, ISBN 978-7-50-283971-0, 2012 (in Chinese).

He, F., Bai, L., Wang, J., Liu, Y., Cai, X., Sun, Y., Zhang, L., Fang, T., and Guo, G.: Deep structure and quaternary activities of the Xiadian fault zone, Seismology and Geology, 35(3), 490-505, https://doi.org/10.3969/j.issn.0253-4967.2013.03.004, 640   2013.

Huang, X., Yang, X., Yang, H., Hu, Z., and Zhang, L.: Re-Evaluating the Surface Rupture and Slip Distribution of the AD 1609 M7 1/4 Hongyapu Earthquake Along the Northern Margin of the Qilian Shan, NW China: Implications for Thrust Fault Rupture Segmentation, Front. Earth Sc.-Switz, 9, 98, https://doi.org/10.3389/feart.2021.633820, 2021a.

Huang, X., Yang, H., Yang, X., Yang, H., Hu, Z., and Zhang, L.: Holocene paleoeseismology of the Fodongmiao-Hongyazi 645   Fault along the Northern Tibetan margin (Western China) and implication to intraplate earthquake rupturing pattern, Tectonophysics, 808, 228812, https://doi.org/10.1016/j.tecto.2021.228812, 2021b.

ITHACA: https://www.isprambiente.gov.it/en/projects/soil-and-territory/italy-hazards-from-capable-faulting-1?set_language=en, last access: 9 March 2024.

Liu, B., Chai, C., Feng, S., Zhao, C., Yuan, H.: Seismic exploration method for buried fault and its up-breakpoint in 650   Quaternary sediment area—An example of Yinchuan buried active fault, Chinese Journal of Geophysics, 51(5), 1475-1483, 2008 (in Chinese).

Lei, Q., Chai, C., Meng, G., Du, P., Wang, Y., Xie, X., Zhang, X.: Composite drilling section exploration of Yinchuan buried fault, Seismology and Geology, 30(1), 250-263, 2008 (in Chinese).

Liang, G. and Wu, Y.: Active fault survey and earthquake hazard assessment in Guangzhou, Science Press, ISBN 978-7-03-655   037757-9, 2013 (in Chinese).

Langridge, R. M., Ries, W. F., Litchfield, N. J., Villamor, P., Van Dissen, R. J., Barrell, D. J. A., Rattenburya, M. S., Herona, D. W., Haubrocka, S., Townsenda, D. B., Leea, J. M., Berrymana, K. R., Nicolc, A., Coxb S. C., Stirling, M. W.: The New Zealand active faults database. New Zeal. J. Geol. Geop., 59(1), 86-96, https://doi.org/10.1080/00288306.2015.1112818, 2016.

660   Li, K., Xu, X., Wei, L., Wang, Q., and Shu, P.: Evidence of long recurrence times and low slip rate along the 1668 Tancheng earthquake fault, Chin Sci Bull, 64, 1168–1178, https://doi.org/10.1360/N972018-00961, 2019.

Ma, X.: Lithospheric dynamics map of China and adjacent sea area (1:4 000 000), 1987 (in Chinese).

Maldonado, V., Contreras, M., Melnick, D.: A comprehensive database of active and potentially-active continental faults in Chile at 1: 25,000 scale. Sci. data, 8(1), 1-13, https://doi.org/10.6084/m9.figshare.13268993, 2021.

665   Nation-scale earthquake intensity zonation map compiling team (NEIZMT): Spatial distribution map of active tectonics and strong earthquakes in China (1:3 000 000), China Earthquake Administration, 1976 (in Chinese).

Nation-scale earthquake intensity zonation map compiling team (NEIZMT): Map of the major tectonic-system activity and strong earthquakes epicentre distribution in China (1:6 000 000), China Earthquake Administration, 1978 (in Chinese).

NEDC: https://data.earthquake.cn/zcfg/index.html, last access: 20 Jan 2023.

670   NEDC (sub-center in IG, CEA): http://datashare.igl.earthquake.cn/map/ActiveFault/introFault.html, last access: 20 Jan 2023.

Pan, J., Liu, B., Zhu, J., Zhang, X., Fang, S., Wang, F., Duan, Y., Xu, Z.: Comparative experiment on seismic sources in high-resolution seismic exploration for urban active faults. Seismology and Geology, 24(4): 533-541, 2002 (in Chinese).

Qu C.: Building to the active tectonic database of China, Seismology and Geology, 30 (1), 298-304, 2008 (in Chinese).

Rong, Y., M.EERI, Xu, X., Jia Cheng, J., Chen, G., Magistrale, H., M.EERI, and Shen, Z.: A probabilistic seismic hazard 675   model for Mainland China, Earthq. Spectra, 36(1_suppl), 181-209, https://doi.org/10.1177/8755293020910754, 2020

Shen, J. and Bo, J.: Active fault survey and earthquake hazard assessment in Songyuan, Seismological Press, ISBN 978-7-5028-4731-9/P(5427), 2016 (in Chinese).

Shu, P., Fang, L., Zheng, Y., Lu, S., Pan, H., Song, F., and Li, S.: Geological Evidence and Characteristics of Activity of the Wuhe-Mingguang Section of Tancheng-Lujiang Fault Zone in Late Pleistocene, Earthquake Research in China, 30(4), 485-680   499, 2016.

Sun, H., He, H., Wei, Z., Shi, F. and Gao, W.: Late Quaternary paleoearthquakes along the northern segment of the Nantinghe fault on the southeastern margin of the Tibetan Plateau. J. Asian Earth Sci., 138, 258-271, https://doi.org/10.1016/j.jseaes.2017.02.023, 2017.

Shi F., He H., Gao W., Sun, H., Wei, Z., Hao, H., Zou J., Sun, W., and Su, P.: Holocene paleoearthquakes on the 685   Tianqiaogou-Huangyangchuan fault in the northeastern boundary fault system of the Tibetan Plateau, J. Asian Earth Sci., 186, 104049, https://doi.org/10.1016/j.jseaes.2019.104049, 2019.

Shu, P., Min, W., Liu, Y., Xu, X., Li, K., Yu, Z., Yang, H., Luo, H., Wei, S., and Fang, L.: Late Quaternary paleoseismology and faulting behavior of the Yilan-Yitong fault zone and implications for seismic hazards of the Tanlu fault zone, eastern China. J. Asian Earth Sci., 201,1-18, https://doi.org/10.1016/j.jseaes.2020.104509, 2020.

690   Shi F., He H., Liu Y., Wei, Z., and Sun, H.: Active Tectonics of the Nantinghe Fault in Southeastern Tibetan Plateau and its Implications for Continental Collision. Front. Earth Sci., 9, 818225, https://doi.org/10.3389/feart.2021.818225, 2022.

Trifonov, V. G.: Active faults in Eurasia: general remarks, Tectonophys., 380, 123–130, https://doi.org/10.1016/j.tecto.2003.09.017,2004.

Tian, S.: Faults Investigation and Evaluation for Seismic Safety Assessment of Nuclear Power Plants, Technology for 695   Earthquake Disaster Prevention, 1(1), 25-30, https://doi.org/10.3969/j.issn.1673-5722.2006.01.004, 2006 (in Chinese).

Valensise, G. and Pantatosti, D., Database of potential sources for earthquakes larger than M 5.5 in Italy. Version 2.0-2001. Italy: N. p., 2001. Web.

Wang, G., Wang, J., Liu, C., Liu, W., Zhang, P., Lin, Y., Zhu, J., Huang, Z., Zhao, Z.: A trial geochemical prospecting for buried active faults in Fuzhou city. Seismology and Geology, 24(4): 593-600, 2002 (in Chinese).

Wang, Y.: Recognition of "The Working guidelines for exploration and seismic risk assessment of active faults in urban areas (on trial)". Seismology and Geology, 26(4): 559-565, 2004 (in Chinese).

Wang, Y., Meng, G., Chai, C., Liu, Q., Du, P., and Xie, X.: The accurate location methods of buried active fault exploration: an example of Luhuatai faults in Yinchuan graben, Seismology and Geology, 37(1), 256, https://doi.org/10.3969/j.issn.0253-4967.2015.20, 2016 (in Chinese).

Wu, Z., Zhou, C., Ma, X., Wang, J., Huang, X., Wu, X., Hu, M., Ha, G., and Liu, J.: Active faults map of China and adjacent sees (1:5 000 000), Geological Publishing House, 2018 (in Chinese).

Wu, X., Du, K., Yu G., Chen, G., Dong, Y., Xu, X., Chen, Z., and Xu, C.: Implementation and future challenges of seismotectonic mapping system for earthquake emergency response, In IOP Conference Series: Earth and Environmental Science, 861(5), p. 052047, 2021.

Williams, J. N., Wedmore, L. N., Scholz, C. A., Kolawole, F., Wright, L. J., Shillington, D. J., Åke Fagereng, Biggs J., Mdala H., Dulanya Z., Mphepo F., Chindandali P. R. N., Werner, M. J.: The Malawi Active Fault Database: An Onshore‐Offshore Database for Regional Assessment of Seismic Hazard and Tectonic Evolution. Geochem., Geophy., Geos., 23(5), e2022GC010425, https://doi.org/10.1029/2022GC010425, 2022.

Wu, X., Xu, C., Xu, X., Chen, G., Zhu, A., Zhang, L., Yu, G., and Du, K.: A Web-GIS hazards information system of the 2008 Wenchuan Earthquake in China, 2, 210-217, Natural Hazards Research, https://doi.org/10.1016/j.nhres.2022.03.003, 2022.

Xu, X. and Deng, Q.: Nonlinear characteristics of paleoseismicity in China. Journal of Geophysical Research: Solid Earth, 101(B3), 6209-6231, https://doi.org/10.1029/95JB01238, 1996.

Xu, X., Ji, F., Yu, G., Chen, W., Wang, F., and Jiang, W.: Reconstrction of paleoearthquake sequence using stratigraphic records from drill logs: a study at the Xiadian Fault, Seismology and Geology, 22(1), 9-19, 2000 (in Chinese).

Xu, X., Yu, G., Ma, W., Ran, Y., Chen, G., Han, Z., Zhang, L., and You, H.: Envidence and methods for determining the safety distance from the potential earthquake surface rupture on active fault, Seismology and Geology, 24(4), 470-483, 2002 (in Chinese).

Xu, X.: Active Faults, Associated Earthquake Disaster Distribution and Policy for Disaster Reduction, Technology for Earthquake Disaster Prevention, 1(1):7-14, https://doi.org/10.3969/j.issn.1673-5722.2006.01.002, 2006 (in Chinese).

Xu, Z., Ji, S., Li, H., Hou, L., Fu, X., and Cai, Z.: Uplift of the Longmenshan range and the Wenchuan earthquake, Episodes, 31, 291-301. https://doi.org/10.18814/epiiugs/2008/v31i3/002, 2008a.

Xu, X., Wen X., Ye J., Ma B., Chen, Zhou, et al, The MS 8.0 Wenchuan Earthquake surface ruptures and its seismogenic structure, Seismology and Geology, 30(3), 597-629, 2008b (in Chinese).

730   Xu, X., Wen, X., Yu, G., Chen, G., Klinger, Y., Hubbard, J., and Shaw, J.: Coseismic reverse- and oblique-slip surface faulting generated by the 2008 Mw 7.9 Wenchuan earthquake, China, Geology, 37(6), 515-518, https://doi.org/10.1130/G25462A.1, 2009a.

Xu, X.: Album of 5.12. Wenchuan MS 8.0 earthquake surface ruptures, China, Seismological Press, ISBN 978-7-5028-3542-2, 2009b (in Chinese).

735   Xu, X., Jiang, G., Yu, G., and Wu X., Zhang J., and Li X.: Discussion on seismogenic fault of the Ludian M_S 6.5 earthquake and its tectonic attribution, Chinese Journal of Geophysics, 57(9), 3060-3068, https://doi.org/10.6038/cjg20140931, 2014a (in Chinese).

Xu, C., Xu, X., Shen, L., Dou, S., Wu, S., Tian, Y., and Li, X.: Inventory of landslides triggered by the 2014 M_S 6.5 Ludian earthquake and its implications on several earthquake parameters, Seismology and Geology, 36(004), 1186-1203,
740   https://doi.org/10.3969/j.issn.0253-4967.2014.04.020, 2014b (in Chinese).

Xu, X., Yu, G., Ran, Y., Yang, X., Zhang, L., Sun, F., Du, W., and Liu, B.: Introduction on urban active faults in China: urban active fault survey achievement in 20 large cities of China, Seismological Press, ISBN 978-7-5028-4410-3, 2015 (in Chinese).

Xu, X., Guo T., Liu S., Yu G., Chen G., Wu X.: Discussion on issues associated with setback distance from active fault.
745   Seismology and Geology, 38(003), 477-502, https://doi.org/10.3969/j.issn.0253-4967.2016.03.001, 2016a (in Chinese).

Xu, X., Han, Z., Yang, X., Zhang, S., Yu, G., Zhou, B., Li, F., Ma, B., Chen, G., and Ran, Y.: Seismotectonic Map in China and its Adjacent Regions (1:4 000 000), Seismological Press, 2016b (in Chinese).

Xu, X., Wu, X., Yu, G., Tan X., Li, K.: Seismo-Geological Signatures for identifying $M \geqq 7.0$ earthquake risk areas and their premilimary application in mainland China, Seismology and Geology, 39(002), 219-275, https://doi.org/10.3969/j.issn.0253-
750   4967.2017.02.001, 2017 (in Chinese).

Xu, X.: China Active Fault Database, Active Fault Survey Data Centre at Institute of Geology, China Earthquake Administration [data set], https://doi.org/10.12031/activefault.china.400.2023.db, 2023.

Yang, F.: Active fault survey and earthquake hazard assessment in Changchun, Seismological Press, ISBN 978-7-5028-3695-5, 2010 (in Chinese).

755   Yoshioka, T., and Miyamoto, F.: Active fault database of Japan: Its construction and search system. In AGU Fall Meeting Abstracts, Vol. 2011, pp. S21A-2144, 2011.

Yang, H., Yang, X., Huang, X., Li, A., Huang, W., and Zhang, L.: New constraints on slip rates of the Fodongmiao-Hongyazi fault in the Northern Qilian Shan, NE Tibet, from the 10Be exposure dating of offset terraces, J. Asian Earth Sci., 151, 131-147, https://dx.doi.org/10.1016/j.jseaes.2017.10.034, 2018a.

760   Yang, H., Yang, X., Zhang, H., Huang, X., Huang, W., and Zhang, N.: Active fold deformation and crustal shortening rates of the Qilian Shan Foreland Thrust Belt, NE Tibet, since the Late Pleistocene. Tectonophysics, 742, 84-100, https://doi.org/10.1016/j.tecto.2018.05.019, 2018b.

Yang, H., Yang, X., Huang, W., Li, A., Hu, Z., Huang, X., and Yang, H.: 10Be and OSL dating of Pleistocene fluvial terraces along the Hongshuiba River: Constraints on tectonic and climatic drivers for fluvial downcutting across the NE
765   Tibetan Plateau margin, China, Geomorphology, 348, 106884, https://doi.org/10.1016/j.geomorph.2019.106884, 2020.

Yeats, R. S., K. Sieh, C. R. Allen: The Geology of Earthquakes, Oxford: Oxford University Press, 1997.

Zelenin, E., Bachmanov, D., Garipova, S., Trifonov, V., and Kozhurin, A.: The Active Faults of Eurasia Database (AFEAD): the ontology and design behind the continental-scale dataset, Earth Syst. Sci. Data, 14, 4489–4503, https://doi.org/10.5194/essd-14-4489-2022, 2022.

770   Zhu, J., Xu, X., and Huang, Z.: Active fault survey and earthquake hazard assessment in Fuzhou, Science Press, https://doi.org/10.3969/j.issn.1001-4683.2005.01.001, 2005 (in Chinese).

Zhang, P., Deng, Q., Zhang, G., Ma, J., Gan, W., Min, W., Mao, F., and Wang, Q.: Active tectonic blocks and strong earthquakes in the continent of China, Sci. China Ser. D, 46(2), 13-24, 2003.